Edward R.T. Tiekink

13 Crystal chemistry of the isomeric N,N′′-bis(pyridin-*n*-ylmethyl)-ethanediamides, *n* = 2, 3 or 4

13.1 Introduction

A working definition for a "multi-component crystal" is a crystal comprising more than one molecular entity with all components present in stoichiometric quantities. This volume, "*Aspects of Multi-Component Crystals: Synthesis, Concepts and Function*", contains many such examples, e.g. solvates, salts and neutral species. Without dispute, co-crystals are attracting greatest attention in the general area of multi-component crystals, comprising molecules that are normally solids under ambient conditions with the co-crystal co-formers (the individual species comprising the multi-component crystal) being in their neutral states. With the latter definition in mind, there are many varied motivations for studying organic co-crystals. These encompass concepts such as modifying luminescence properties, developing new non-linear optical materials, chiral resolution, promoting crystallisation of otherwise uncrystallisable species and the stabilisation of unusual/unstable molecules. In addition to these considerations, the area undoubtedly attracting the most interest is the development of new pharmaceuticals based on co-crystal technology. Recently published reviews provide excellent introductions to the field [1–3].

Molecules that featured in early systematic co-crystallisation investigations form the focus of this chapter; namely the isomeric N,N′-bis(pyridin-*n*-ylmethyl)ethanediamides, $n = 2, 3$ or 4, which are abbreviated as $^{2}LH_2$, $^{3}LH_2$ and $^{4}LH_2$ respectively. As seen from Figure 13.1, these molecules feature diamide moieties, located centrally, flanked by terminal pyridyl rings differing in the location of the pyridyl-N atoms. The presence of these functional groups makes them ideally suited to form co-crystals stabilised by hydrogen and/or halogen bonding. The purpose of this overview is to demonstrate the variety and complexity of co-crystals formed by these compounds. This is complemented by a brief overview of the complexing ability of $^{2}LH_2$, $^{3}LH_2$ and $^{4}LH_2$ and some protonated/deprotonated forms of these towards metal centres, both transition metals and main group elements. This allows both correlations with all-organic analogues and provides clues to the capabilities and versatility of these multi-functional molecules/ions.

The ensuing discussion is broken down as follows: First, a description of available structures of parent molecules is provided. An overview of the co-crystals formed by $^{2}LH_2$ is then presented, then any salts, followed by complexation patterns to metals in

https://doi.org/10.1515/9783110464955-013

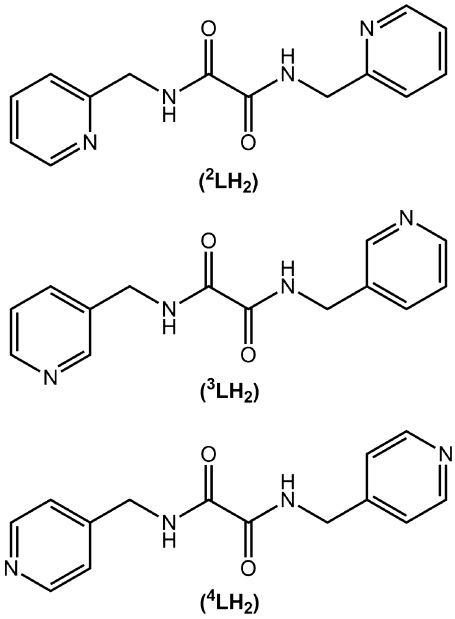

Fig. 13.1: Chemical diagrams for isomeric N,N′-bis(pyridin-*n*-ylmethyl)ethanediamides, $n = 2$, 3 and 4, showing the abbreviations employed for each isomer.

neutral form and ionic forms. The subsequent sections cover the structural chemistry of the higher homologues, $^{3}LH_2$ and $^{4}LH_2$.

Data, in the form of crystallographic information files (CIFs), were extracted from the Cambridge Crystallographic Database [4] and interrogated using PLATON [5]. Diagrams were drawn using DIAMOND [6]. Structures with unresolvable disorders were not included. However, if the disorder was associated with "spectator" species, e.g. counter-ions, solvent, etc., and an analysis of the intermolecular interactions/coordinating ability of $^{n}LH_2$ was possible, the structure was retained in this review. No other restrictions were applied.

In the case of all-organic species, the focus of the discussion is upon the nature of interactions involving the heteroatoms and of their metal complexes upon the co-ordinating sites, meaning that complete descriptions of the overall molecular packing for most species is beyond the scope of this survey. Rather, the focus of the discussion for metal-containing species is upon the supramolecular association of $^{n}LH_2$ and derived ionic species via hydrogen bonding interactions.

13.2 Crystal chemistry of $^{2}LH_2$, $^{3}LH_2$ and $^{4}LH_2$

Although the crystal structure of $^{2}LH_2$ has yet to be reported, two polymorphs are known for each of $^{3}LH_2$ [7] and $^{4}LH_2$ [8, 9]. The dithiodiamide analogue of $^{2}LH_2$ has been described and based on the experimental and theoretical (DFT) structures. It

was suggested that an all planar conformation located about a centre of inversion is most stable owing to the presence of intramolecular amide-N–H···N(pyridyl) hydrogen bonding [10]. With these observations in mind, it is quite possible that a similar conformation such as centrosymmetric planar applies to $^{2}LH_2$.

The two polymorphs of $^{3}LH_2$ have only just recently been described [8], and each crystallises in the monoclinic space group $P2_1/c$. In form I, one entire molecule comprises the asymmetric unit, i.e. $Z' = 1$, whereas in form II there are two independent molecules, each located about a centre of inversion, i.e. $Z' = 2 \times 0.5$. An overlay of the three molecules is shown in Figure 13.2, from which it is apparent that although the central cores are coincident, the relative orientations of the pyridyl rings differ significantly.

Although the emphasis of this chapter is supramolecular chemistry, here, a brief description of the salient features of the central core is given, as these are common to the all-organic structures described herein. For example, their coordination to metals often results in significant differences as highlighted in the relevant sections. The diamide moiety is usually strictly planar with rarely only minor deviations apparent. The arrangement is always anti-periplanar, facilitating the formation of intramolecular amide-N–H···O(amide) hydrogen bonds. Calculations (DFT) show that alternative arrangements are more than 6 kcal mmol^{-1} less stable [8]. Finally, being attached to two electronegative substituents, the amide-C–C(amide) bond is usually longer than anticipated for an sp^2-C–C(sp^2) bond [5]. The striking difference between the polymorphs of $^{3}LH_2$ relates to the disposition of the pyridyl rings, being syn-periplanar in form I and anti-periplanar in both independent molecules in form II. Furthermore, in form I, the pyridyl-N atoms are orientated to the same side of the molecule. However, the observed conformational flexibility does not have great energy significance, as computational chemistry (DFT) shows the differences in energy for the different conformations to be less than 1–2 kcal mol^{-1}, thereby allowing for the adoption of different molecular packing arrangements, which can be quite distinct.

The intermolecular interactions involving the heteroatoms in form I of $^{3}LH_2$ leads to a supramolecular layer Figure 13.3a, with the corrugated topology related to the

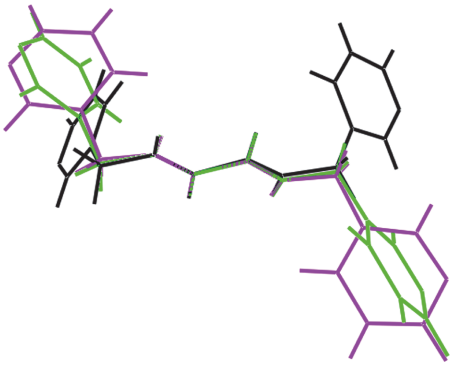

Fig. 13.2: An overlay diagram for the three independent molecules for $^{2}LH_2$: form I (*black image*) and form II (*green and pink*). The molecules have been overlapped so that the central chromophores are coincident.

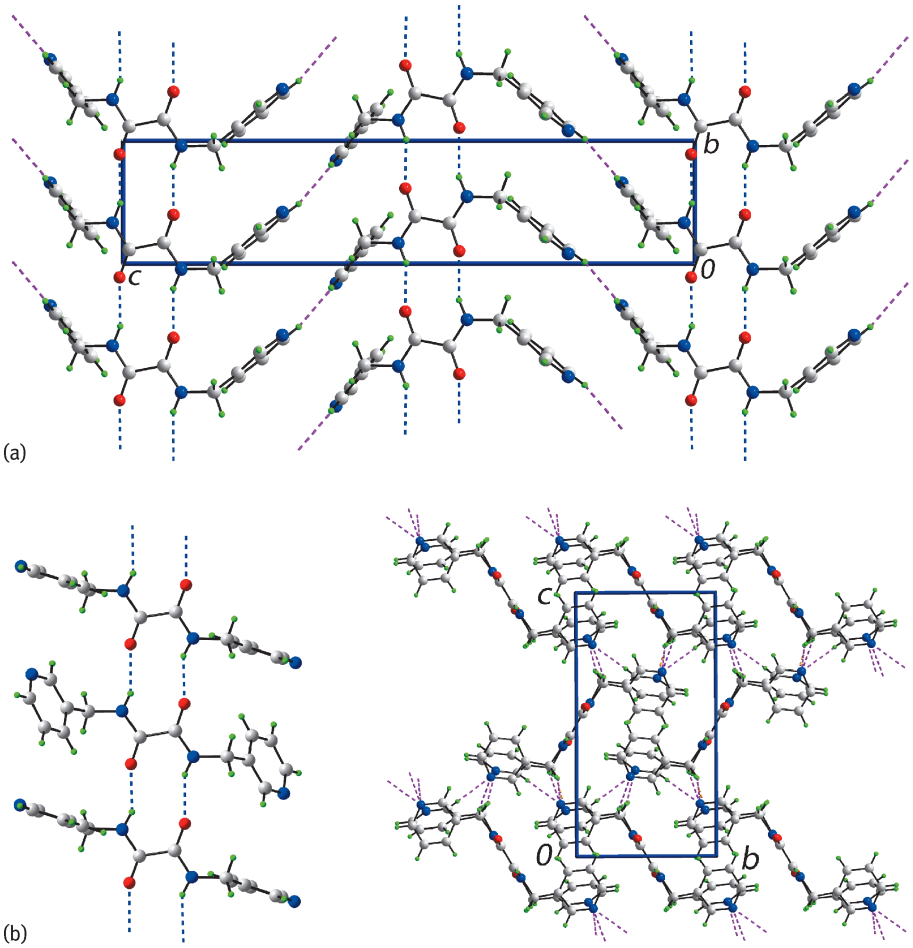

Fig. 13.3: (a) Molecular packing for $^{3}LH_2$, form I, showing the supramolecular layer in the bc plane, and (b) and (c) molecular packing for $^{2}LH_2$, form II, showing the supramolecular tape and view of the unit cell contents in projection down the a-axis respectively. The amide-N–H···O(amide) hydrogen bonds are shown as *blue dashed lines* whereas the C–H···N(pyridyl) interactions are shown as *pink dashed lines*.

syn-periplanar disposition of the pyridyl rings. The main feature of the molecular packing is the formation of supramolecular tapes involving both amide moieties and strong amide-N–H···O(amide) hydrogen bonds leading to 10-membered $\{\cdots HNC_2O\}_2$ synthons. The tapes are connected into a two-dimensional arrangement by pyridyl-C–H···N(pyridyl) interactions, involving two pyridyl rings but one pyridyl-N atom only as the other pyridyl-N atom does not form an intermolecular interaction within the standard distance criteria assumed in PLATON [5]. Supramolecular tapes, akin to those of form I, are found in the crystal of form II (Figure 13.3b, left), and comprise

alternating independent molecules. The tapes are consolidated into the three-dimensional packing by pyridyl- and methylene C–H···N(pyridyl) interactions involving both molecules (Figure 13.3b, right). Two pyridyl-N atoms do not form significant intermolecular interactions.

As mentioned above, two polymorphs are found for $^{4}LH_2$ with, in a sense, the opposite characteristics of forms I and II of $^{3}LH_2$. That is, although both forms of $^{4}LH_2$ are monoclinic, in form I of $^{4}LH_2$ [9], two independent molecules, neither with symmetry, comprise the asymmetric unit, i.e. $Z' = 2$, whereas in form II [10], which is also monoclinic, the molecule lies about a centre of inversion, i.e. $Z' = 0.5$. A common feature of each molecule is the anti-periplanar disposition of the pyridyl rings, but, as seen in the overlay diagram of Figure 13.4, in each of the molecules the pyridyl rings have distinct orientations with respect to the central diamide moiety. In the second independent molecule of form I, the twist about the central amide-C–C(amide) is significantly greater, at about 5º, than is normally observed in non-coordinating $^{n}LH_2$ molecules discussed herein (see green image in Figure 13.4).

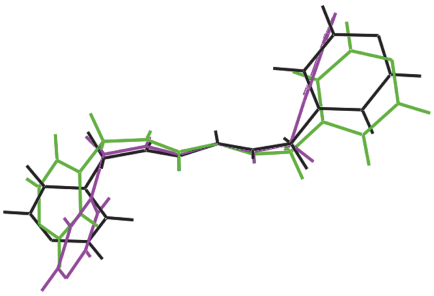

Fig. 13.4: An overlay diagram for the three independent molecules for $^{2}LH_2$: form I (black and green images) and form II (pink). The molecules have been overlapped so that the central chromophores are coincident.

The molecular packing in the two polymorphic forms of $^{4}LH_2$ differ greatly. In form I [9], the two independent molecules associate into dimeric aggregates via the 10-membered amide synthon, $\{\ldots HNC_2O\}_2$. The exocyclic amide groups associate with pyridyl-N, i.e. via amide-N–H···N(pyridyl) hydrogen bonds, so that a supramolecular layer is formed (Figure 13.5a). The topology is cross-linked. In this hydrogen bonding scheme there are no apparent roles for the amide-O and half the available pyridyl-N atoms. The presence of pyridyl-C–H···O(amide) interactions, with each amide-O atom accepting two such interactions, link the layers into the three-dimensional crystal (Figure 13.5b).

Supramolecular layers sustained by hydrogen bonding are also evident in the crystal of form II of $^{4}LH_2$ [10] (Figure 13.6a). However these, with a sinusoidal topology, are sustained exclusively by amide-N–H···N(pyridyl) hydrogen bonding. The layers are linked by pyridyl-C–H···O(amide) contacts (Figure 13.6b). Clearly, in the two forms of $^{4}LH_2$, there is a trade-off between utilising half or all available pyridyl-N atoms in the hydrogen bonding scheme, forming amide $\{\ldots HNC_2O\}_2$ synthons and compensating C–H···O(amide) interactions.

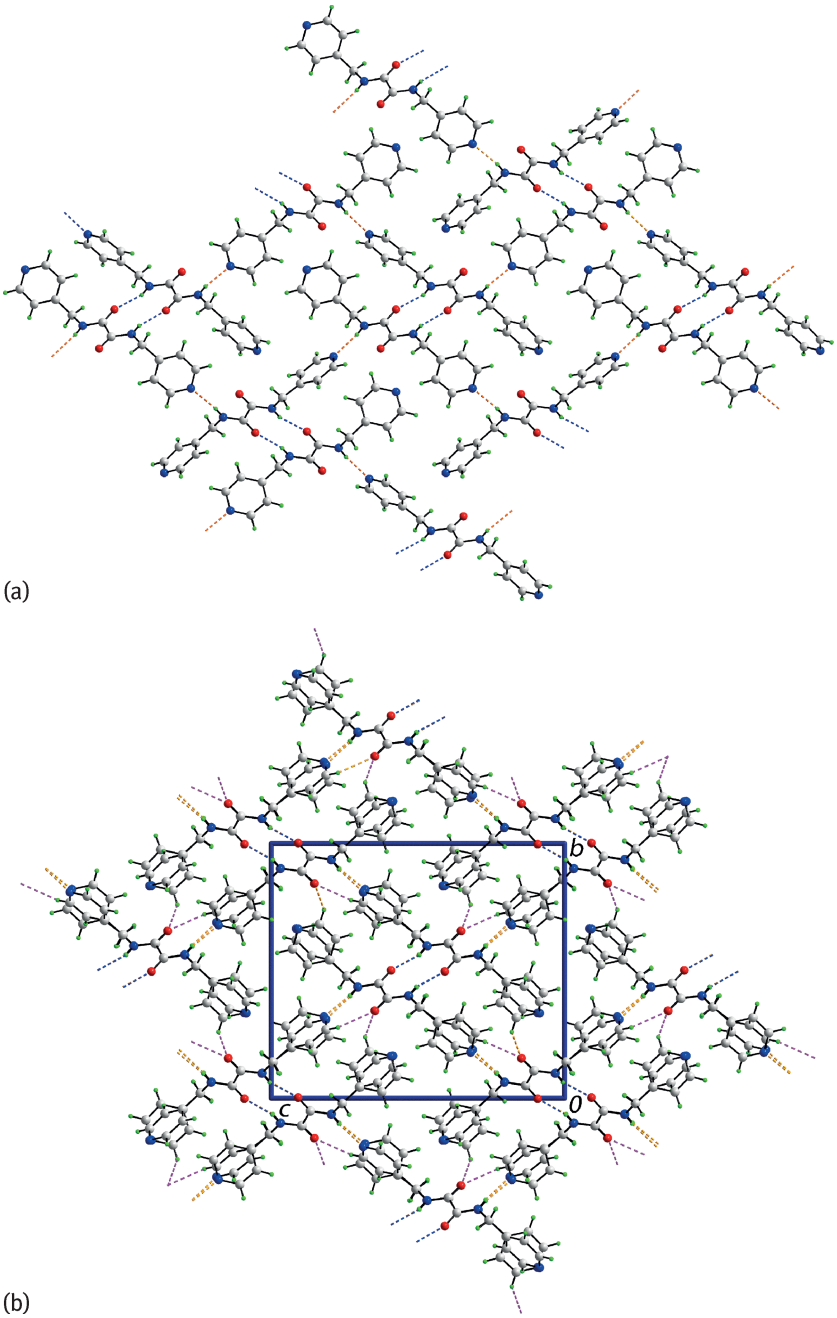

Fig. 13.5: Molecular packing for $^{4}LH_2$, form I, showing the (a) supramolecular layer in the bc-plane, and (b) view of the unit cell contents in projection down the a-axis. The amide-N–H···O(amide) and amide-N–H···N(pyridyl) interactions are shown as *blue and orange dashed lines* respectively, whereas the pyridyl-C–H···O(amide) interactions are shown as *pink dashed lines*.

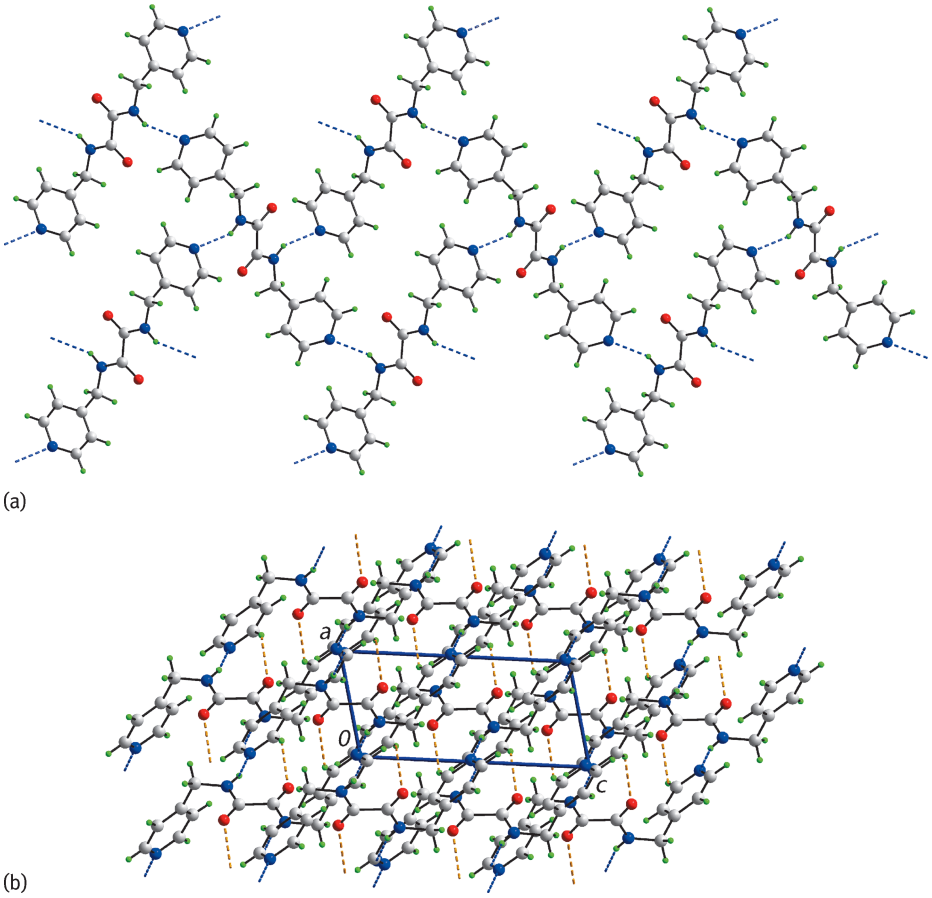

Fig. 13.6: Molecular packing for $^{4}LH_2$, form II, showing (a) the supramolecular layer in the bc plane, and (b) the view of the unit cell contents in projection down the b-axis. The amide-N–H···N(pyridyl) and C–H···O(amide) interactions are shown as *blue and pink dashed lines*, respectively.

13.3 Multi-component crystals of $^{2}LH_2$ and derivatives

In keeping with the lack of structural data for $^{2}LH_2$, there is a paucity of structural data for co-crystals/salts involving this isomer. By contrast, there are well over ten coordination compounds containing $^{2}LH_2$ and ions derived from this. A thorough analysis of the hydrogen bonding patterns of the all-organic species is presented. However, only a summary of key coordination modes and, when applicable, hydrogen bonding involving $^{2}LH_2$/ions derived from $^{2}LH_2$ is included for the metal containing species.

13.3.1 Co-crystal

There is a sole example of a co-crystal involving $^{2}LH_2$, namely a 1 : 2 co-crystal with 2-aminobenzoic acid and $^{2}LH_2$ [11]. As $^{2}LH_2$ lies about a centre of inversion, there is only one unique acid molecule. The key feature of the supramolecular association is the formation of a layer, whereby the pyridyl-N atoms are connected to carboxylic acids via hydroxyl-O–H···N(pyridyl) hydrogen bonds and a seven-membered {C(=O)OH…NCH} heterosynthon. This brings about a pyridyl-C–H···O(carbonyl) interaction, which is well known for being robust in co-crystal technology [12]. The amino group is pivotal in the molecular packing by donating, via amino-N–H···O(amide), and accepting, via amide-N–H···N(amino), hydrogen bonds leading to 14-membered $\{\cdots NH\cdots OC_2NH\}_2$ synthons (Figure 13.7). The layers are connected by pyridyl-C–H···O(amide, carbonyl) interactions to consolidate the crystal.

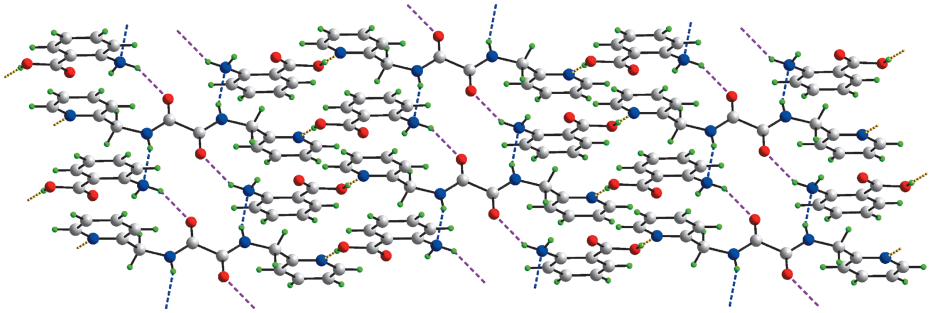

Fig. 13.7: Supramolecular layer in the 1 : 2 co-crystal formed between $^{2}LH_2$ and 2-aminobenzic acid, with hydroxyl-O–H···N(pyridyl), amide-N–H···O(amide) and amino-N–H···N(amino) hydrogen bonds shown as *orange*, *blue* and *pink dashed lines* respectively.

13.3.2 Salts

There are two salts in the crystallographic literature with each anion derived from benzoic acid derivatives. The first salt to be described is a 1 : 2 salt between $[^{2}LH_4]^{2+}$ and 3,5-dicarboxybenzoate [13], where the centrosymmetric cation is doubly protonated at the pyridyl-N atoms, i.e. $[^{2}LH_4]^{2+}$ is a dipyridinium di-cation. The di-cations associate into a supramolecular tape with translational symmetry via a sequence of amide $\{\ldots HNC_2O\}_2$ synthons akin to that shown in Figure 13.3a for form I of $^{3}LH_2$ [8]. As illustrated in Figure 13.8a, the tapes are connected into a three-dimensional architecture by charge-assisted pyridinium-N–H···O(carboxylate) and hydroxyl-O–H···O(carboxylate) hydrogen bonds, in addition to eight-membered carboxylic acid dimer $\{\ldots HOCO\}_2$ synthons.

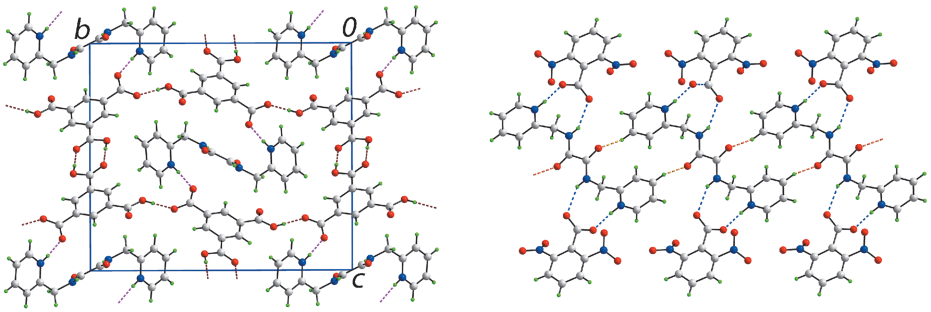

(a) (b)

Fig. 13.8: (a) A view of the unit cell contents in projection down the a-axis in the 1 : 2 salt: $[^2LH_4]^{2+}$ and 3,5-dicarboxbenzoate. The amide tapes along the a-axis are connected by hydroxyl-O–H···O(carboxylate) and pyridinium-N–H···O(carboxylate) hydrogen bonds shown as *brown and pink dashed lines* respectively, and (b) supramolecular layer in the 1 : 2 salt: $[^2LH_4]^{2+}$ and 2,6-dinitobenzoate. The amide- and pyridinium-N–H···O(carboxylate) and pyridyl-C–H···O(amide) interactions are shown as *blue and orange dashed lines* respectively.

The second salt also has a 1 : 2 stoichiometry and is found between $[^2LH_4]^{2+}$ and 2,6-dinitrobenzoate and again, owing to the di-cation being centrosymmetric, there is only one independent anion in the asymmetric unit [14]. Charge-assisted hydrogen bonding also features in the crystal, whereby the carboxylate groups span adjacent pyridinium-N–H and amide-N–H groups to form a nine-membered heterosynthon $\{\ldots HNC_2NH\cdots OCO\}$. The resulting three-ion but electrically neutral aggregate associates with symmetry-related neighbours via pyridyl-C–H···O(amide) interactions to form a supramolecular layer, as shown in Figure 13.8b.

13.3.3 Metal containing species

There are three examples in the literature where $^2LH_2$ coordinates in the neutral mode and, curiously, each displays a distinctive mode of coordination. In the centrosymmetric six-coordinate dimethylplatinum(IV) di-cationic complex [15], where the platinum is further coordinated by a 2,2′-bipyridyl-type ligand and a 4-caroxybenzyl group, the $^2LH_2$ molecule is bidentate, bridging via the pyridyl-N atoms (Figure 13.9a). As the diamide chromophore is flanked on either side by bulky substituents, it does not participate in hydrogen bonding interactions. The terminal carboxylic acid groups associate via $\{\ldots HOCO\}_2$ synthons to form a supramolecular chain (not illustrated). In the mononuclear compound $HgI_2(^2LH_2)_2$ [16], both $^2LH_2$ molecules coordinate in the monodentate mode (Figure 13.9b), with the pendent pyridyl-N atoms participating in neither coordination nor hydrogen bonding interactions. However, each of the independent $^2LH_2$ molecules self-associates to form amide tapes, via $\{\ldots HNC_2O\}_2$ synthons, with the result that a supramolecular tube is con-

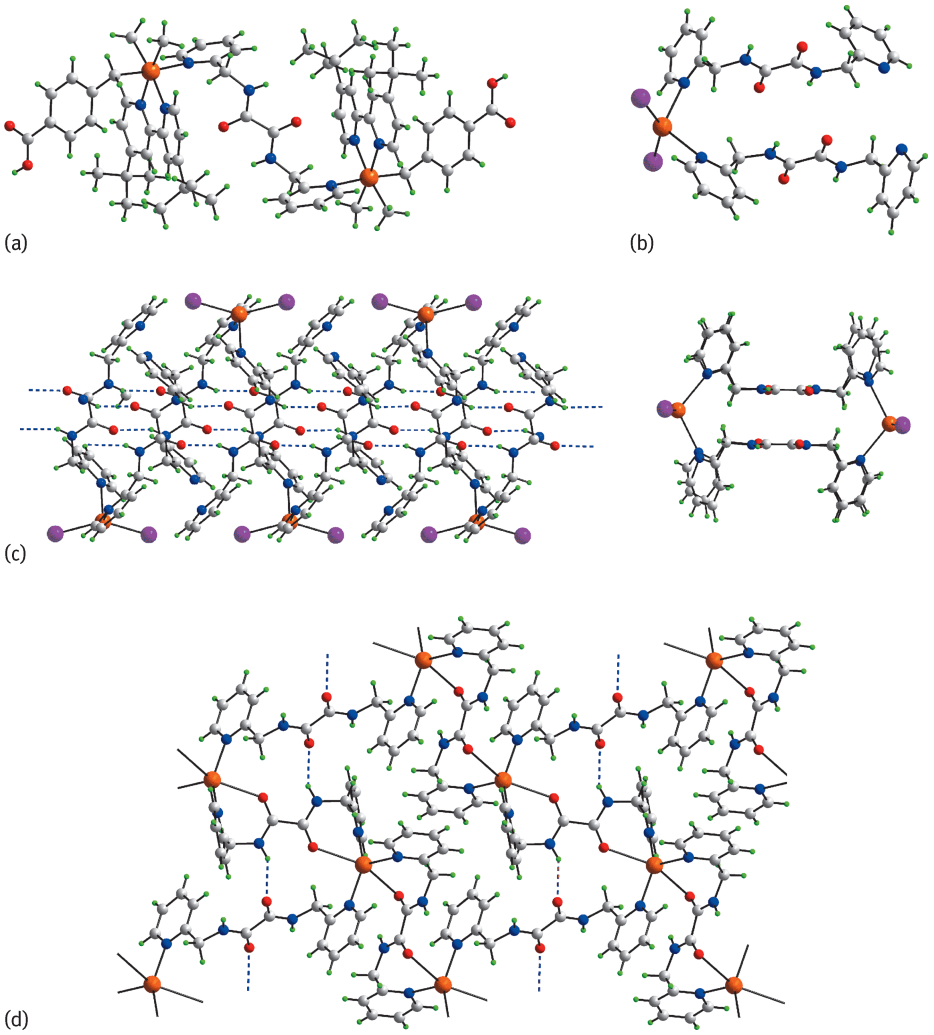

Fig. 13.9: Neutral coordination mode for $^2LH_2$. (a) A bridging mode via pyridyl-N atoms in a dicationic dimethylplatinum(IV) complex, (b) the asymmetric unit in $HgI_2(^2LH_2)_2$ shown as a monodentate mode of coordination via a single pyridyl-N atom, (c) side-on and end-on views of the supramolecular tube in $HgI_2(^2LH_2)_2$ mediated by amide-N–H···O(amide) hydrogen bonding (*blue dashed lines*), and (d) both bidentate (pyridyl-N) and tetradentate (pyridyl-N and amide-O) bridging modes in sheets of $[Ag_2(^2LH_2)_3^{2+}]_n$.

structed (as shown in the side- and end-on views of Figure 13.9c). The third structure is the most interesting of all three and, in fact, displays two distinct coordination modes. In $\{Ag_2(^2LH_2)_3(\text{trifluoromethanesulfonate})_2\}_n$ [17] and referring to Figure 13.8d, the silver ions are connected into a two-dimensional grid via one bidentate bridging $^2LH_2$ molecule, coordinating via both pyridyl-N atoms, and two

tetradentate $^2LH_2$ molecules, which employ all pyridyl-N and amide-O atoms in coordination. The tetradentate coordinate mode results in the formation of seven-membered Ag–N–C–C–N–C–O chelate rings. Further stability to the array is provided by amide-N–H···O(amide) hydrogen bonds between bi- and tetra-dentate coordinating ligands. The acidic sites not involved in the construction of the aforementioned layer are connected to the trifluoromethanesulfonate anions via amide-N–N···O(trifluoromethanesulfonate) hydrogen bonding to contribute to the stabilisation between layers.

The remaining six structures available in the literature feature the $[^2L]^{2-}$ di-anion [18–21]. In the mononuclear and neutral complex Pd(^{2}L) (Figure 13.10a), the $[^2L]^{2-}$ di-anion wraps around the palladium(II) centre to define a square planar geometry defined by the four nitrogen atoms [18]. In the di-cation of $[(DMF)_2Cu(^2L)Cu(DMF)_2](ClO_4)_2$ (Figure 13.10b), $[^2L]^{2-}$ is hexadentate, employing all six heteroatoms in co-

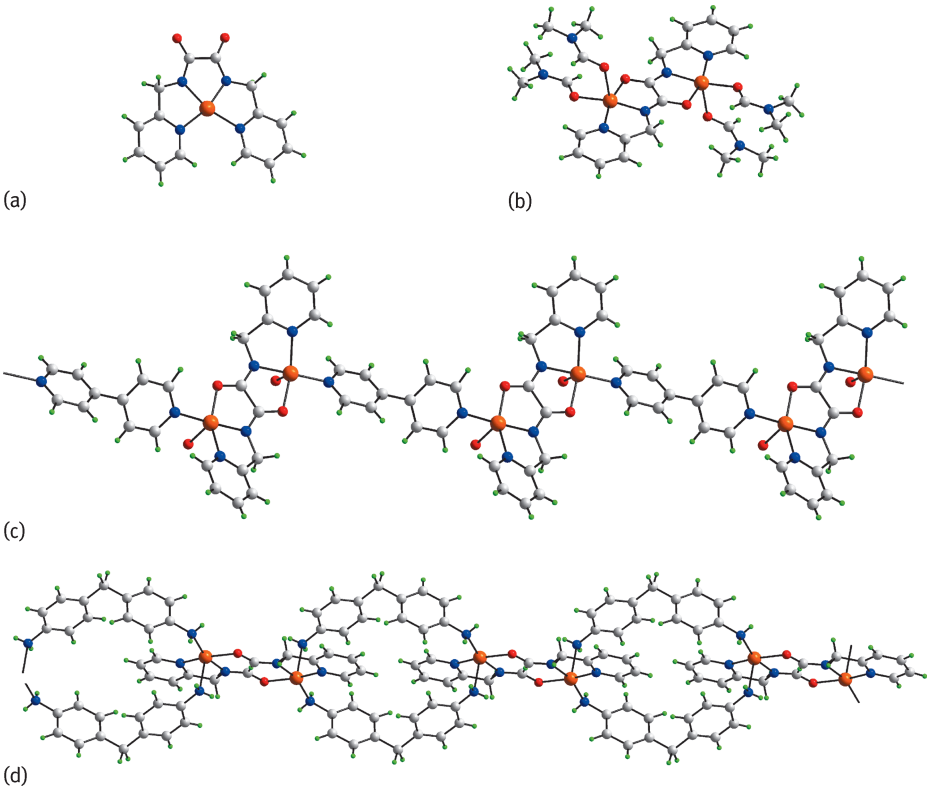

Fig. 13.10: (a) A tetradentate-N_4 coordination mode for $[^2L]^{2-}$ in Pd(^{2}L), (b) a hexadentate N_4O_2 coordination mode for $[^2L]^{2-}$ in $[(DMF)_2Cu(oxalate)Cu(DMF)_2]^{2+}$, (c) and (d) hexadentate N_4O_2 coordination modes for $[^2L]^{2-}$ leading to a coordination polymers in each of (c) $\{(H_2O)Cu(^2L)Cu(OH_2)(4,4'-bipyridyl)^{2+}\}_n$ and (d) $\{Cu(^2L)Cu[bis(4-aminophenyl)methyl]_2^{2+}\}_n$.

ordination with two copper(II) atoms [19]. DMF is *N*, *N*-dimethylformamide. A similar coordination mode is found in each of the next two structures whereby similar binuclear units of the [Cu(^{2}L)Cu] di-cation, described above, are linked into coordination polymers by bridging 4,4′-bipyridyl ligands, $\{[(H_2O)Cu(^2L)Cu(OH_2)(4,4'-bipyridyl)](NO_3)_2\}_n$ (Figure 13.10c), or two bis(4-aminophenyl)methyl ligands in $[\{Cu(^2L)Cu[bis(4-aminophenyl)methyl]_2\}(NO_3)_2]_n$ (Figure 13.10d), giving a chain of loops, whereby the coordinated water molecules of $\{[(H_2O)Cu(^2L)Cu(OH_2)(4,4'-bipyridyl)](NO_3)_2\}_n$ are displaced [20].

13.4 Multi-component crystals of $^3LH_2$ and derivatives

Significantly more examples of $^3LH_2$/ions in the forms of co-crystals, salts and metal containing species have been reported compared with the $^2LH_2$ isomer described in the previous section. Noteworthy is the observation of co-crystals stabilised by halogen bonding, a mono-protonated form, $[^3LH_3]^+$, in addition to a tautomeric form of the $^3LH_2$ structure shown in Figure 13.1.

13.4.1 Co-crystals

Co-crystals involving $^3LH_2$ fall into two classes, namely involving carboxylic acids and halogens, with the former described first. Reflecting the propensity of carboxylic acids to associate with pyridyl-N, the 1 : 2 co-crystal comprising $^3LH_2$ and 4-nitrobenzoic assemble into a three-molecule aggregate. $^3LH_2$ is located about a centre of the inversion [22]. As shown in Figure 13.11a, the aggregates are linked into a supramolecular ladder as the amide-N–H atom forms a hydrogen bond with a nitro-O atom. The role of the amide-O atom is to participate in three C–H···O interactions, one hydrogen being derived from a phenyl ring and two from pyridyl rings. These sustain a two-dimensional double layer (Figure 13.11a, lower image). The $^3LH_2$ molecule in its 1 : 2 co-crystal with 2-aminobenzoic acid accepts two hydroxyl-O–H···N(pyridyl) and two amino-N–H···O(amide) hydrogen bonds. At the same time, it donates two amide-N–H···O(carbonyl) hydrogen bonds and is thereby surrounded by six 2-aminobenzoic acid molecules [11], indicating that $^3LH_2$ is saturated in terms of its hydrogen bonding capacity (Figure 13.11b). The hydrogen bonding extends in three dimensions to generate the supramolecular architecture (Figure 13.11c).

The next co-crystal to be described is the 1 : 1 co-crystal between $^3LH_2$ and the bi-functional carboxylic acid, 2,2′-disulfanediyldibenzoic acid [23]. As is evident from Figure 13.11d, a supramolecular tape of linked 10-membered $\{\ldots HNC_2O\}_2$ synthons is formed with the pendant pyridyl-N atoms bridged by the carboxylic acid groups via hydroxyl-O–H···N(pyridyl) hydrogen bonds.

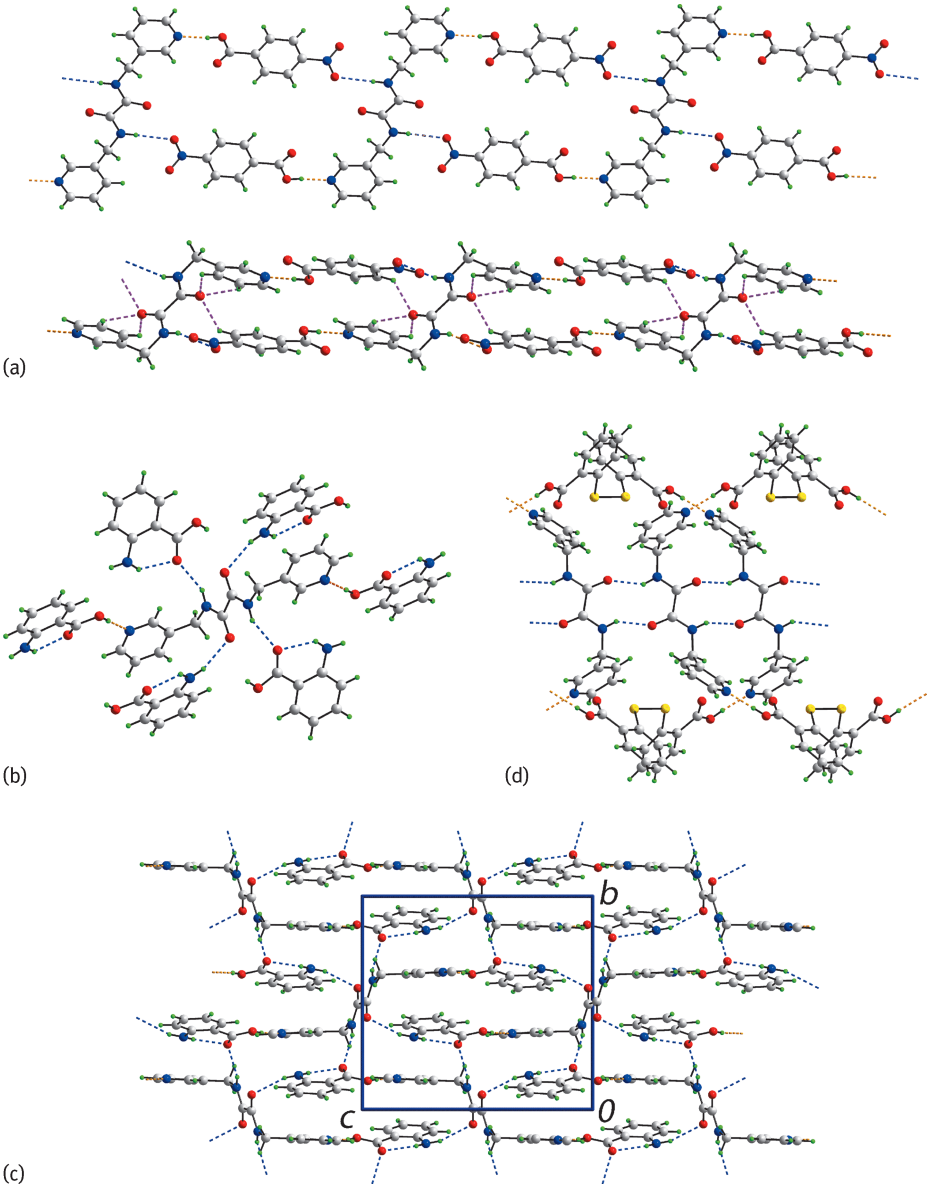

Fig. 13.11: (a) Supramolecular aggregation in the 1 : 2 co-crystal formed between $^3LH_2$ and 4-nitrobenzoic acid: ladder and double layer, (b) hydrogen-bonding interactions involving $^3LH_2$ and 2-aminobenzoic acid in the 1 : 2 co-crystal, showing the immediate environment about one $^3LH_2$ molecule, (c) showing the overall three-dimensional architecture, and (d) a supramolecular chain in the 1 : 1 co-crystal comprising $^3LH_2$ and 2,2′-disulfanediyldibenzoic acid. The hydroxyl-O–H···N(pyridyl) and amide/amine-N–H···O hydrogen bonds are shown as *orange and blue dashed lines* respectively.

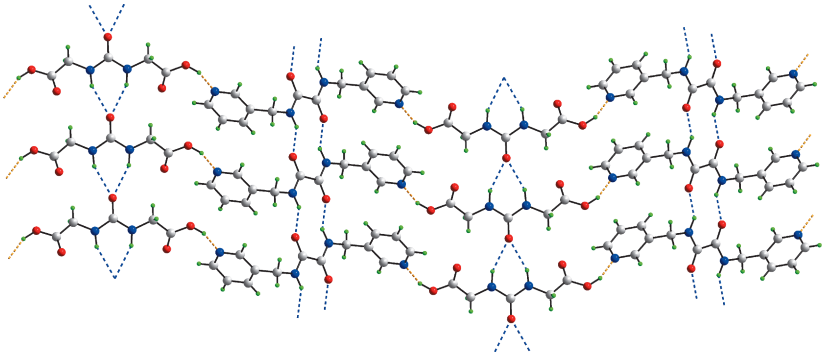

Fig. 13.12: Supramolecular layer in the 1 : 1 co-crystal of $^{3}LH_2$ with N,N′-dicarboxymethylurea. The hydroxyl-O–H···N(pyridyl) and amide-N–H···O hydrogen bonds are shown as *orange and blue dashed lines* respectively.

In the 1 : 1 co-crystal of $^{3}LH_2$ with N,N′-dicarboxymethylurea [24], supramolecular tapes mediated by ten-membered amide synthons, $\{\ldots HNC_2O\}_2$, are formed by $^{3}LH_2$. Related tapes are formed by the N,N′-dicarboxymethylurea molecules as a result

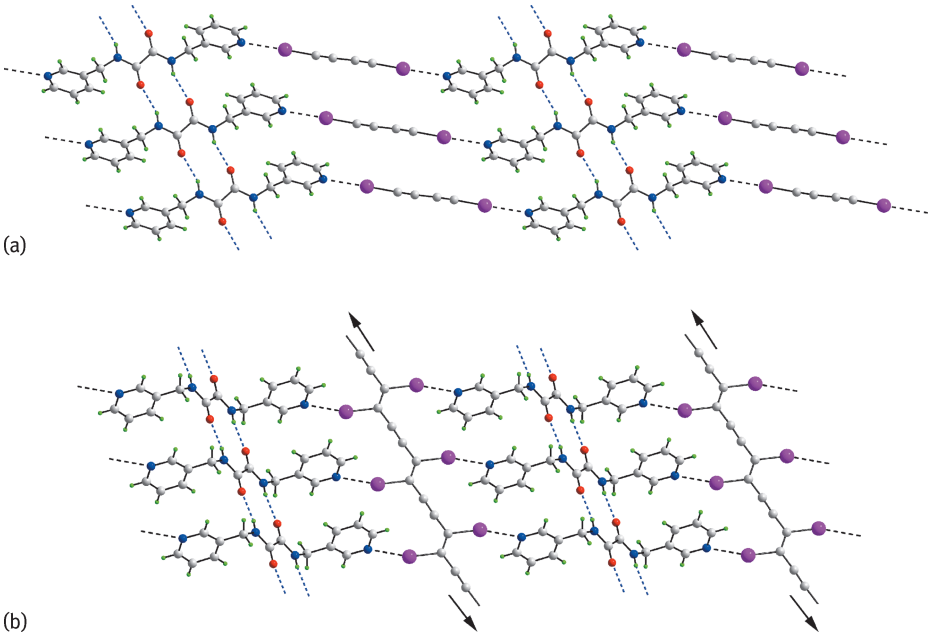

Fig. 13.13: Combination of hydrogen and N···I halogen bonding leading to two-dimensional arrays in 1 : 1 co-crystals of $^{3}LH_2$ with (a) 1,4-di-iodobuta-1,3-diyne and (b) polymeric hemi-kis(iododiacetylene). The amide-N–H···O(amide) hydrogen bonding and halogen bonding are shown as *blue and black dashed lines* respectively.

of urea-N–H···O(carbonyl) hydrogen bonds via six-membered {…O···HNCNH} synthons as the carbonyl-O atom accepts two hydrogen bonds (Figure 13.12). Hydrogen bond links between the chains are hydroxyl-O–H···N(pyridyl), resulting in a two-dimensional array. A similar array is found in the related 1 : 1 co-crystal with N,N′-diglycine oxamide, whereby chains of amide tapes formed by each of the co-crystal co-formers are linked by hydroxyl-O–H···N(pyridyl) hydrogen bonds [24].

As mentioned in the preamble to this chapter, isomeric $^{n}LH_2$ molecules featured in early co-crystal investigations were based on halogen bonding. In this context, there are five co-crystals of $^{3}LH_2$ in the literature featuring halogen bonding [25–28] and four of these adopt similar two-dimensional arrays. One such array is illustrated for the 1 : 1 co-crystal formed between $^{3}LH_2$ and 1,4-di-iodobuta-1,3-diyne [25], where $^{3}LH_2$ molecules are linked into supramolecular tapes via 10-membered $\{\ldots HNC_2O\}_2$ synthons. These, in turn, are linked laterally by N···I halogen bonding, as illustrated in Figure 13.13a. More recently, a 1 : 1 co-crystal of $^{3}LH_2$ with a polymer was described, namely with hemikis(iododiacetylene) (Figure 13.13b) [26]. As mentioned above in the Introduction (Section 13.1), unstable molecules can be stabilised by co-crystal formation and this is realised in the 1 : 1 co-crystal formed between $^{3}LH_2$ and 1,4-dibromobuta-1,3-diyne [27].

In contrast, supramolecular aggregation in the 1 : 1 co-crystal formed between $^{3}LH_2$ and 2,3,5,6-tetrafluoro-1,4-di-iodobenzene is quite distinct from the co-crystal structures just described, with each co-former being centrosymmetric [28]. This struc-

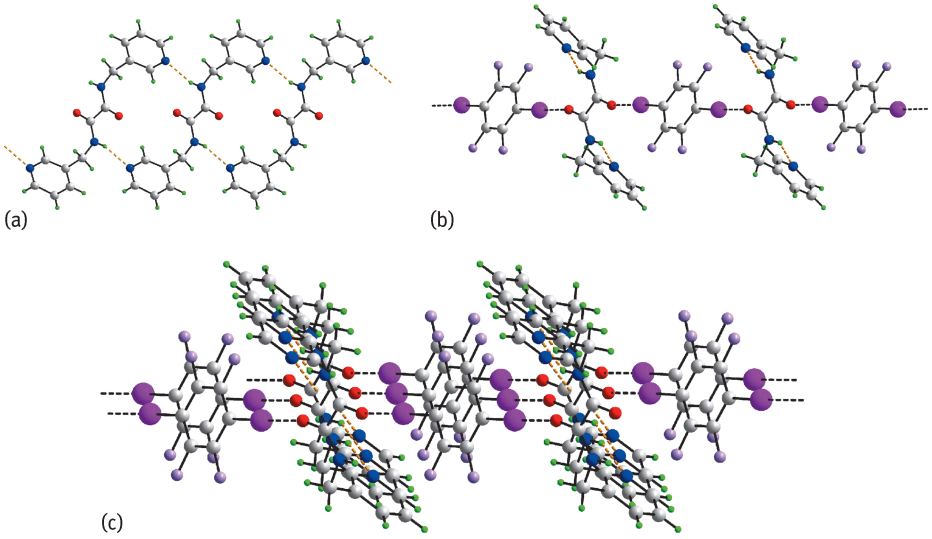

Fig. 13.14: Supramolecular aggregation in the 1 : 1 co-crystal of $^{3}LH_2$ with 2,3,5,6-tetrafluoro-1,4-di-iodobenzene: (a) supramolecular tape sustained by amide-N–H···N(pyridyl) hydrogen bonds, (b) chain sustained by O···I halogen bonding and (c) two-dimensional array. The amide-N–H···N(pyridyl) hydrogen bonding and halogen bonding are shown as *orange and black dashed lines* respectively.

ture is unusual in that, while translationally related molecules of $^3LH_2$ self-assemble into linear supramolecular chains, the association is via amide-N–H···N(pyridyl) hydrogen bonds (Figure 13.14a) resulting in 18-membered $\{\ldots HNC_2NC_3N\}_2$ synthons. This arrangement frees up the amide-O atoms to form O···I halogen bonds, leading to supramolecular chains (Figure 13.14b). The net result is a two-dimensional array, as shown in Figure 13.14c.

13.4.2 Salts

A single example of a salt derived from $^3LH_2$ is known, namely between $[^3LH_4]^{2+}$ and two equivalents of 2,6-dinitrobenzoate [14]. As the di-cation lacks symmetry, two independent anions are found in the asymmetric unit and each forms quite distinct interactions with the di-cation. The di-cation is protonated at each pyridyl-N atom. One carboxylate group bridges the amide-N–H and pyridinium-N–H atoms derived from two molecules and through the application of a centre of inversion, 20-membered $\{\ldots OCO\cdots HNC_3NH\ldots\}_2$ synthons arise from these interactions. The second carboxylate group bridges the equivalent atoms as just described, but employs a single oxygen atom only, with the result that smaller 18-membered $\{\ldots O\cdots HNC_3NH\ldots\}_2$ synthons are formed. The supramolecular assembly arising from the hydrogen bonding is a chain as illustrated in Figure 13.14TS.26. The benzoate atom not participating in the hydrogen bonding scheme just described participates in C–H···O interactions, which, along with other C–H···O(nitro) contacts, consolidates the molecular packing in three dimensions.

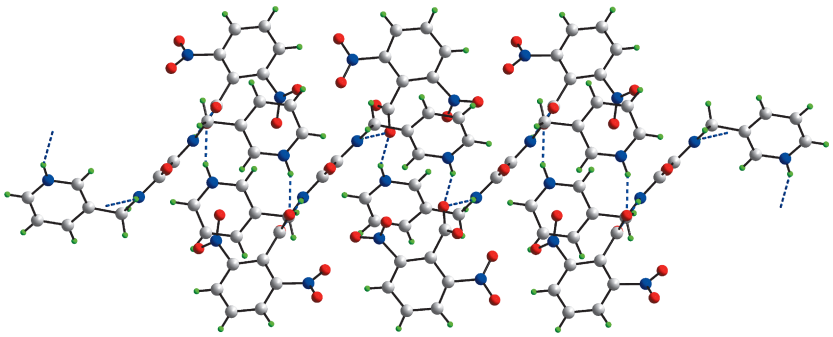

Fig. 13.15: Supramolecular chain in the 1 : 2 salt formed between $[^3LH_4]^{2+}$ and 2,6-dinitrobenzoate. The amide-N–H···O(carboxylate) and charge-assisted pyridinium-N–H···O(carboxylate) hydrogen bonds are shown as *blue dashed lines*.

TS.26 Figure 13.15?

13.4.3 Metal-containing species

A number of metal complexes of $^3LH_2$ and derivatives are available. Several of these feature a bidentate (bridging mode exemplified in Figure 13.16a), whereby two $Zn[S_2CN(Me)CH_2CH_2OH]_2$ entities are linked by $^3LH_2$, utilising both pyridyl-N atoms [29]. In the molecular packing, the $Zn[S_2CN(Me)CH_2CH_2OH]_2$ residues associate about a centre of inversion via hydroxyl-O–H···O(hydroxyl) hydrogen bonds, leading to supramolecular chains and open 28-membered $\{\ldots HOC_2NCSZnSCNC_2O\}_2$ synthons. The voids defined by the aforementioned synthons are sufficiently large to accommodate centrosymmetrically related chains whereby the $^3LH_2$ ligands of one chain thread through the cavities of the other to form a doubly interpenetrated chain, as shown in Figure 13.16b. Similar bridging modes for $^3LH_2$ are found in binuclear complexes where the pendant groups are Zn(phthalocyaninato) complexes with the bulky nature of the terminal residues precluding supramolecular association involving the diamide functionality [30]. In another binuclear complex, two $^3LH_2$ molecules link two palladium(II) centres in the centrosymmetric, tetra-positive cation $[(dppm)Pd(^3LH_2)_2Pd(dppm)]^{4+}$ [31]; dppm is $Ph_2PCH_2PPh_2$. Within the bridging region, there are intramolecular amide-N–H···O(amide) hydrogen bonds, leading to a 10-membered $\{\ldots HNC_2O\}_2$ synthon. The exocyclic amide-N–H atoms form hydrogen bonds to oxygen atoms of trifluoromethanesulfonate anions. In adducts of binuclear $[Co(oxalate)]_2$, i.e. $\{[Co(oxalate)(^3LH_2)]_2\}_n$, each octahedral cobalt centre forms two Co–N(pyridyl) bonds derived from two bidentate, bridging $^3LH_2$ ligands to form a two-dimensional array [32].

In an unprecedented example of a tautomeric form of $^3LH_2$, the dimine-dihydroxyl tautomer, i.e. $3\text{-}NC_5H_4CH_2N{=}C(OH){-}C(OH){=}NCH_2C_5H_4N$, is observed in its 1 : 2 adduct with $Zn[S_2CN(Me)CH_2CH_2OH]_2$, i.e. a tautomer of the structure shown in Figure 13.16a [29]. As shown in Figure 13.16c, the overall molecular conformations of the two structures are comparable. Indeed, similar inter-woven double chains are again found, but this time mediated by hydroxyl-O–H···N(imine) hydrogen bonds. In a variation on the above, the $[^3LH_4]^{2+}$ di-cation can also function as a bidentate, bridging ligand. Thus, in the supramolecular chain of $\{[^3LH_2][EuCl^3(OH_2)]\}_n$ [33] (Figure 13.16d), $[^3LH_4]^{2+}$ employs the amide-O atoms in linking successive europium atoms. The charge balance is provided by non-coordinating chloride anions.

The final three structures to be described in this section also feature bidentate, bridging $^3LH_2$ ligands [16, 34]. A view of one of these, i.e. $\{[Ag(^3LH_2)_2]BF_4\}_n$ [34], is illustrated in Figure 13.17. Each $^3LH_2$ ligand is bidentate, bridging with the resulting N_4 donor set for silver(I), defining a tetrahedral geometry. The molecules are assembled into a three-dimensional array by linear tapes of interlinked $\{\ldots HNC_2O\}_2$ synthons (not evident in Figure 13.17). This arrangement leads to cross-like channels in which reside the BF_4^- anions. A very similar structure is found in the nitrate analogue [34]. To a first approximation, a similar three-dimensional architecture is found in $\{[Cu(^3LH_2)_2Br].Br.H_2O\}_n$ [16]. Each of the $^3LH_2$ and coordinated bromide ligands

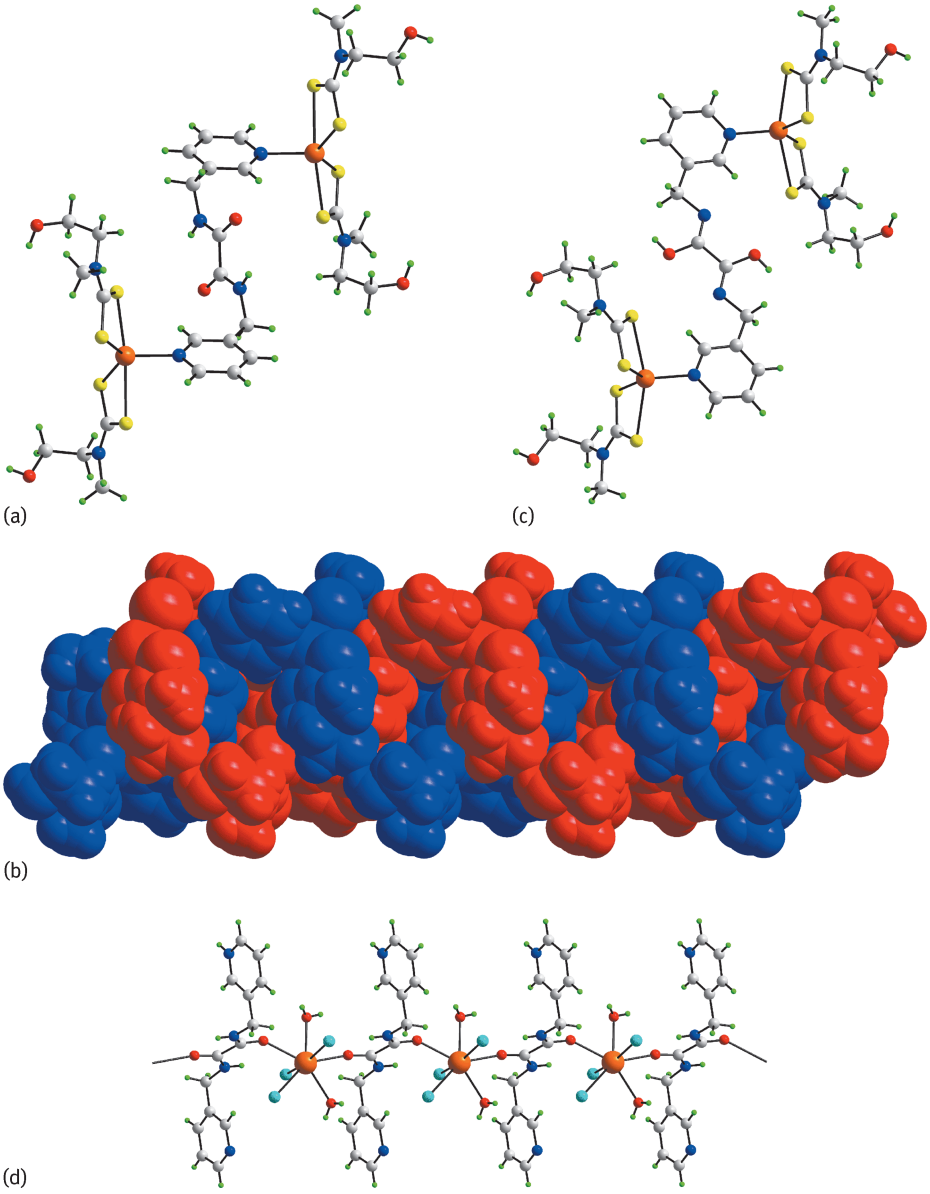

Fig. 13.16: Bidentate, bridging modes for $[^3LH_2]$ and derivatives: (a) $[^3LH_2]$ bridging two $Zn[S_2CN(Me)CH_2CH_2OH]_2$ entities, (b) interwoven double chains from the supramolecular chain formed by the molecule shown in (a), (c) imine-hydroxyl tautomeric form of $[^3LH_2]$, bridging two $Zn[S_2CN(Me)CH_2CH_2OH]_2$ entities, and (d) $[^3LH_4]^{2+}$ bridging $[EuCl_3(OH_2)]^-$ anions within a chain.

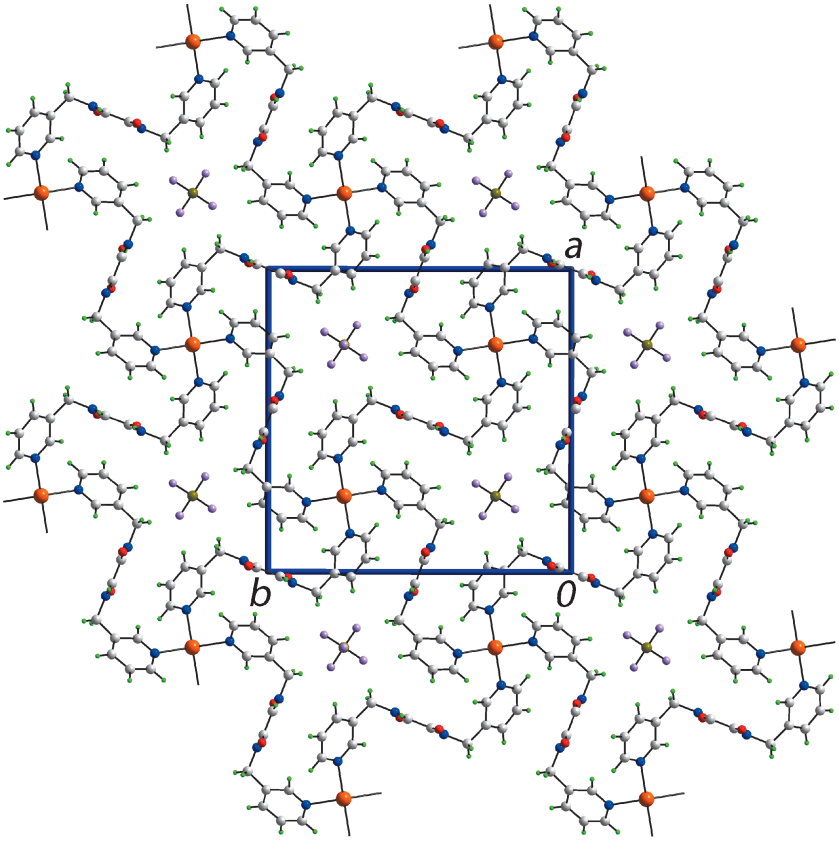

Fig. 13.17: A view of the three-dimensional architecture showing in projection down the *c*-axis in the structure of $\{[Ag(^{3}LH_2)_2]BF_4\}_n$.

is bidentate-bridging leading to trans-Br_2N_4 coordination geometries for copper(II). The formation of diamide tapes, mediated by $\{\ldots HNC_2O\}_2$ synthons, reinforces the Cu–Br–Cu bridges.

13.5 Multi-component crystals of $^{4}LH_2$ and derivatives

The most frequently studied of the isomeric $^{n}LH_2$ molecules by far is the one with $n = 4$. As with the previous section, co-crystals are described first followed by salts and then metal-containing species. The discussion on co-crystals begins with those involving carboxylic acids, then hydroxyl-containing molecules and finally, those that form halogen-bonding interactions.

13.5.1 Co-crystals

There are five co-crystals in the literature involving $^4LH_2$ and carboxylic acids, one of which is a monofunctional carboxylic acid [14] and the other four are bifunctional, having two carboxylic acid residues [24, 35, 36]. In the former, $^4LH_2$ is located about a centre of inversion and so in this 1 : 2 co-crystal, there is one independent molecule of (4-nitrophenyl)acetic acid [14]. As might now be anticipated based on related structures described earlier, a three-molecule aggregate is formed, which is stabilised by hydroxyl-O–H···N(pyridyl) hydrogen bonding. These aggregates are linked into a linear supramolecular chain via amide-N–H···O(hydroxyl) hydrogen bonds leading to the formation of 14-membered $\{\ldots HNC_4N\}_2$ synthons (Figure 13.18). The amide-O forms a weak C–H···O interaction within the chain.

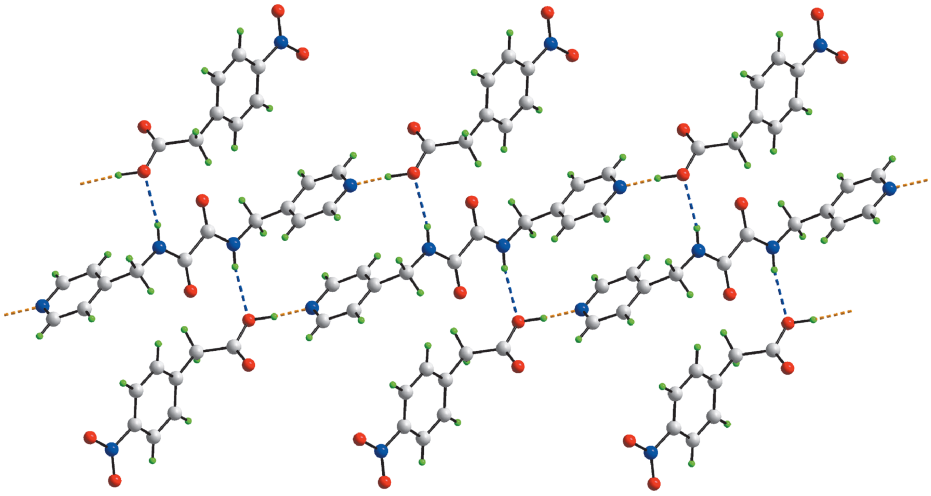

Fig. 13.18: Supramolecular chain in the 2 : 1 co-crystal of [$^4LH_2$] with (4-nitrophenyl)acetic acid. The hydroxyl-O–H···N(pyridyl) and amide-N–H···O(hydroxyl) hydrogen bonds are shown as *orange and blue dashed lines* respectively.

The common features of the remaining 1 : 1 co-crystals containing bifunctional carboxylic acids are the formation of amide tapes, via 10-membered $\{\ldots HNC_2O\}_2$ synthons, and the formation of hydroxyl-O–H···N(pyridyl) hydrogen bonding, which links the tapes into two-dimensional arrays. In the co-crystal with N,N′-bis(carboxymethyl) urea [35], the urea molecules are connected by urea-N–H···O(carbonyl) hydrogen bonds (Figure 13.19a), whereas in the co-crystals with N,N′-bis(2-hydroxymethyl)oxalamide (Figure 13.19b) and N,N′-bis(2-hydroxyethyl)oxalamide [35], the links between each of these co-formers are also of the type amide-N–H···O(amide). In an interesting variation, a polymer, namely poly(1,2-bis(2-carboxyethyl)tetra-1-en-3-yn-1,4-diyl, provides the bridges between amide tapes (Figure 13.19c) [36].

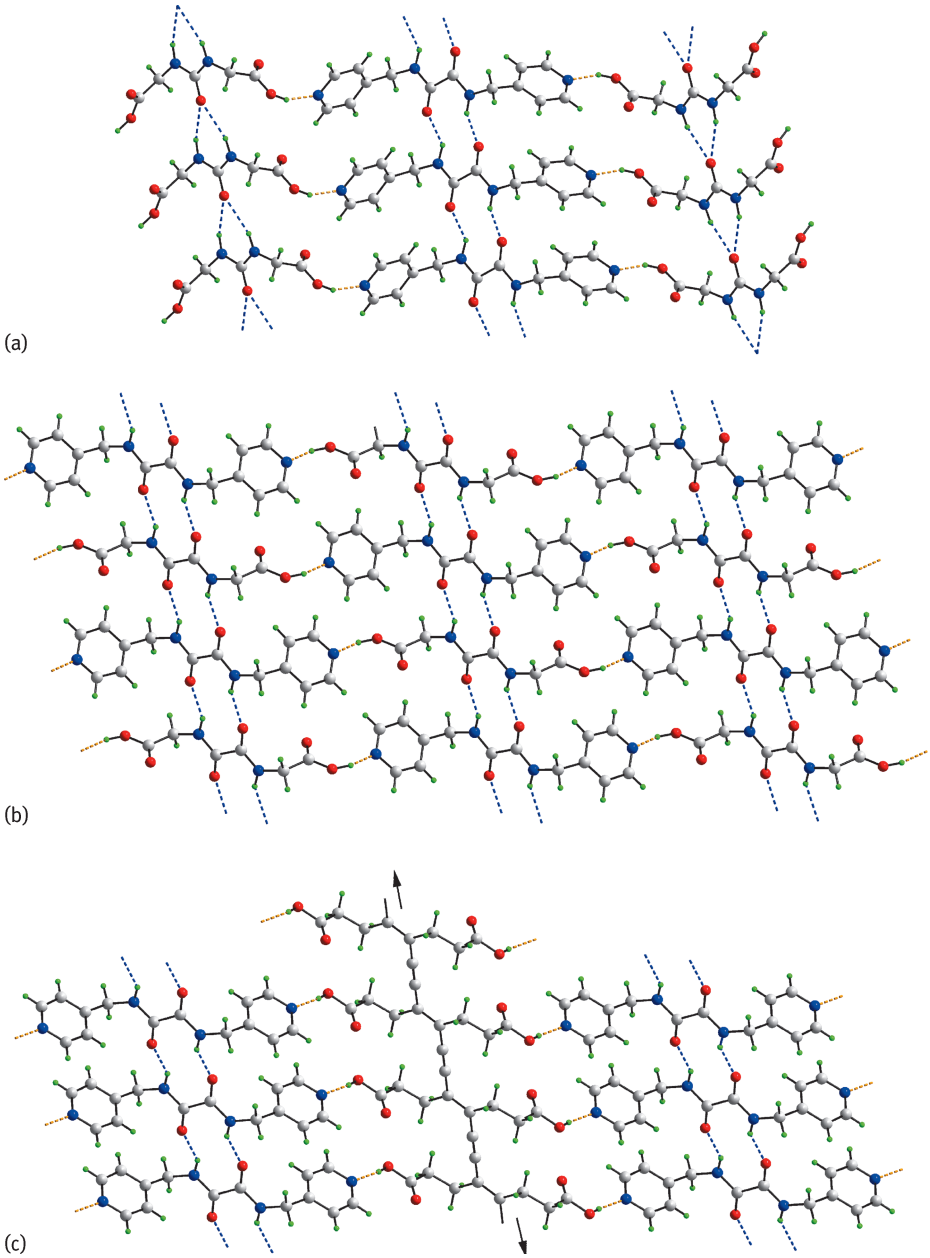

Fig. 13.19: Two-dimensional supramolecular arrays of 1 : 1 co-crystals of [$^4LH_2$] with (a) N,N′-bis(carboxymethyl)urea, (b) N,N′-bis(2-hydroxymethyl)oxalamide and (c) poly(1,2-bis(2-carboxyethyl)tetra-1-en-3-yn-1,4-diyl. The hydroxyl-O–H···N(pyridyl) and amide-N–H···O(amide) hydrogen bonds are shown as *orange and blue dashed lines* respectively. In (a), the amide-N–H···O(carbonyl) hydrogen bonds are shown as *blue dashed lines*.

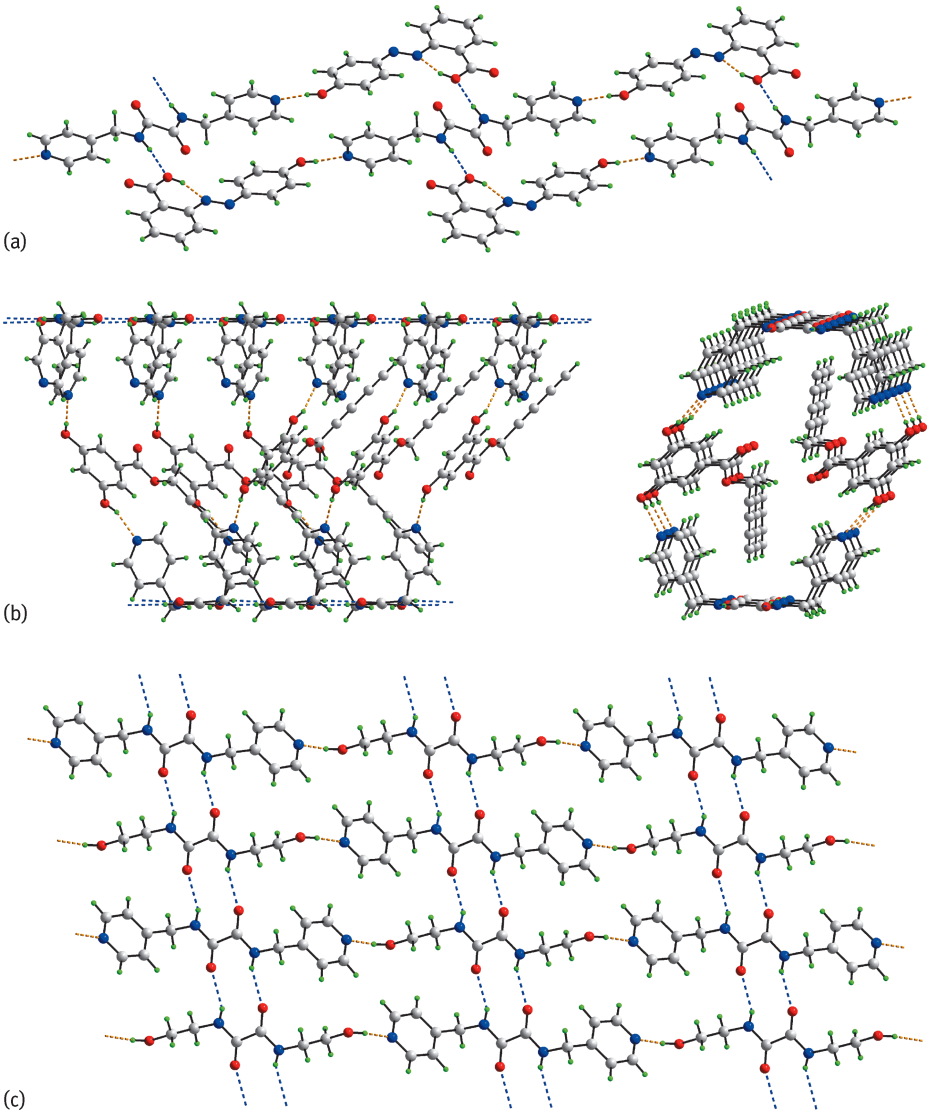

Fig. 13.20: Supramolecular association in co-crystals of [^{4}LH$_2$]: (a) 1 : 2 with bis(2-((4-hydroxyphenyl)diazenyl)benzoic acid), (b) 1 : 1 with penta-2,4-diynyl 3,5-dihydroxybenzoate and (c) 1 : 1 with N,N′-bis(2-hydroxyethyl)oxalamide. The hydroxyl-O–H···N(pyridyl) and hydroxyl-O–H···N(azo) hydrogen bonds are shown as *orange dashed lines* and the amide-N-H···O(hydroxyl) and amide-N–H···O(amide) hydrogen bonding are shown as *blue dashed lines*.

There are four structures where the co-former with ^{4}LH$_2$ has hydroxyl substituents and these are discussed next as a group. The 1 : 2 co-crystal formed with 2-[(4-hydroxyphenyl)diazenyl]benzoic acid, both hydroxyl and carboxylic acid residues, are present

in the co-former [37], thereby providing a nice segue between the previously described co-crystal structures and those under consideration here. This structure is particularly notable for the absence of the hydroxyl-O–H···N(pyridyl) hydrogen bonding normally observed in the carboxylic acid co-crystal structures described herein. Instead, an intramolecular hydroxyl-O–H···N(azo) hydrogen bond is formed to close a six-membered loop. Links between the co-formers are hydrogen bonds of the type hydroxyl-O–H···N(pyridyl) and amide-N–H···O(hydroxyl), so that comparatively large 40-membered $\{\ldots HNC_2NC_4N\cdots HOC_4N_2\ldots HO\}_2$ synthons are formed (Figure 13.20a). The supramolecular assembly arising from the specified hydrogen bonding is a linear supramolecular chain; the amide-O atom does not form a significant intermolecular contact. Two very similar architectures are found in 1 : 1 co-crystals with penta-2,4-diynyl 3,5-dihydroxybenzoate (Figure 13.20b), and with the polymer, poly(penta-2,4-diynyl) [38]. In the crystal of the former, the pyridyl rings adopt, to a first approximation, a syn-periplanar conformation and associate into amide tapes via $\{\ldots HNC_2O\}_2$ synthons. Two such tapes are connected by hydroxyl-O–H···N(pyridyl) hydrogen bonds to generate a supramolecular tube, propagated by a 2_1 screw axis, as shown in the two views of Figure 13.20b. Linear, supramolecular amide tapes mediated by $\{\ldots HNC_2O\}_2$ synthons are also found in the fourth co-crystal in this sub-category; namely the 1 : 1 co-crystal between $^4LH_2$ and N,N′-bis(2-hydroxyethyl)oxalamide [35].

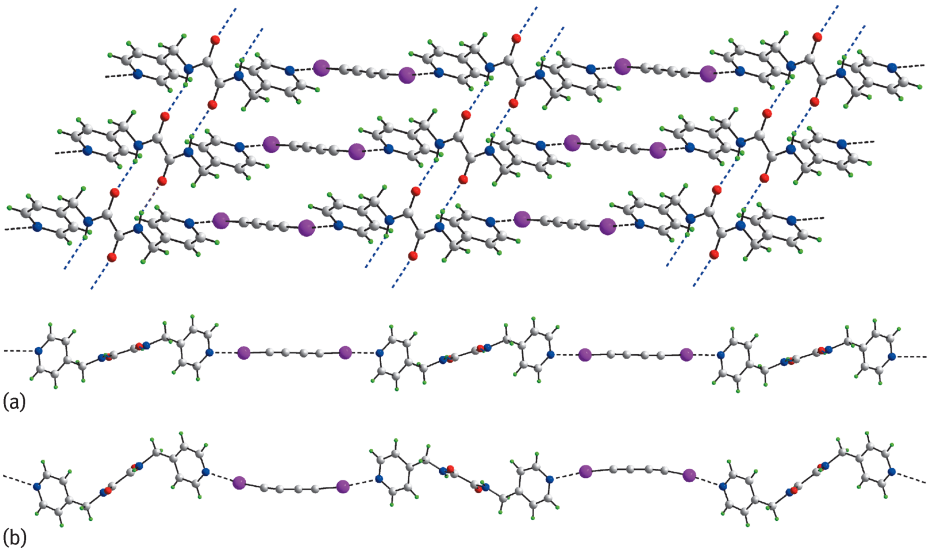

Fig. 13.21: Supramolecular aggregation in the 1 : 1 co-crystals of $^4LH_2$ with 1,4-di-iodobuta-1,3-diyne: (a) planar and side-on views of the two-dimensional array sustained by amide-N–H···O(amide) hydrogen bonds and I···N halogen bonds on the co-crystal determined at 3 GPa, and (b) side-on view of the same co-crystal determined under ambient conditions. The amide-N–H···O(amide) hydrogen bonding and halogen bonding are shown as *blue and black dashed lines* respectively.

For the closely related di-carboxylic acid analogues described above, the tapes are connected into two-dimensional arrays by hydroxyl-O–H···N(pyridyl) hydrogen bonding, with each tape mediated by amide-N–H···O(amide) hydrogen bonding and $\{\ldots HNCO\}_2$ synthons, as shown in Figure 13.20c.

Two 1 : 1 co-crystals sustained by both hydrogen bonding and halogen bonding have been described above, i.e. with 1,4-di-iodobuta-1,3-diyne [25, 39] and with 1,6-di-iodohexa-1,3,5-triyne [25]. These closely resemble the supramolecular association in analogues formed with $^3LH_2$. The former is of particular interest as the structure has been determined under ambient and high pressure (3 GPa) conditions. Two views of the supramolecular aggregation are shown in Figure 13.21a, from which it can be seen that the two-dimensional array is clearly flatter in the high-pressure form than that determined under normal pressure conditions (Figure 13.21b) [25].

13.5.2 Salts

Two salts, both containing $[^4LH_4]^{2+}$ di-cations, have been reported [10, 14]. In the di-nitrate salt (Figure 13.22a) where the di-cations are centrosymmetric, charge-assisted pyridinium-N–H···O(nitrate) and amide-N–H···O(nitrate) hydrogen bonds are evident [10]. In essence, the nitrate anion employs one oxygen atom to bridge symmetry-related molecules so that a three-dimensional architecture ensues. Although there is no formal role for the amide-O atoms in this scheme, it is noted that these form close contacts with pyridinium-C–H hydrogen atoms. In the second salt, the $[^4LH_4]^{2+}$ di-cations are also located about a centre of inversion and similar charge-assisted hydrogen bonding is observed to that just described, but involving a single benzoate-oxygen atom only, i.e. pyridinium-N–H···O(benzoate) and amide-N–H···O(benzoate) hydrogen bonds, leading to 22-membered $\{\ldots HNC_2NC_4NH\}_2$ synthons [14]. This contrasts with the more open arrangement in $[^4LH_4][NO_3]_2$ [10], resulting in a linear supramolecular chain that is formed instead, with a flat topology (Figure 13.22b). The amide-O atoms form very weak contacts with pyridinium-C–H hydrogen atoms.

13.5.3 Metal containing species

The coordination chemistry of $^4LH_2$ is relatively simple compared with those exhibited by the $^2LH_2$ and $^3LH_2$ isomers in that it is restricted, with one exception, to bidentate bridging coordination modes. This bridging mode is clearly illustrated in Figure 13.23a for the di-cation in $[Ph_3PAu(^4LH_2)AuPPh_3][ClO_4]_2$ [40]. The presence of charge-assisted amide-N–H···O(perchlorate) hydrogen bonding restricts further supramolecular association between $^4LH_2$ entities. In the same way, steric effects in a congested zinc porphyrinate complex restrict supramolecular association involving $^4LH_2$ [30]. In a binuclear six-coordinate dimethylplatinum(IV) di-cationic

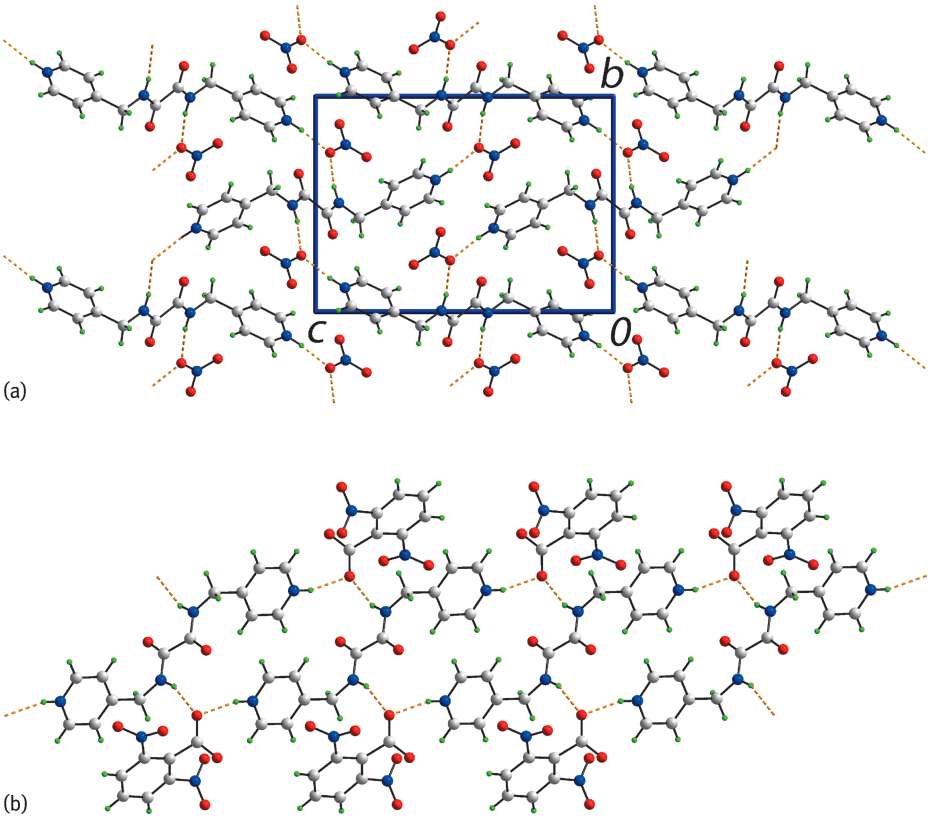

Fig. 13.22: Supramolecular association in salts of $[^4LH_4]^{2+}$. (a) 1 : 2 salt with nitrate, and (b) 1 : 2 salt with 2,6-dinitrobenzoate. The charge-assisted N–H···O hydrogen bonds are shown as *orange dashed lines*.

complex [15], the platinum atoms are bridged by a $^4LH_2$ molecule (Figure 13.23b). Each platinum centre is also coordinated by a 2,2′-bipyridyl-type ligand and a 4-caroxybenzyl group. In this case, the diamide is accessible for hydrogen bonding and forms a $\{\ldots HNC_2O\}_2$ synthon via hydrogen bonds. The terminal 4-caroxybenzyl groups also self-associate via the carboxylic acid synthon, $\{\ldots HOC_2O\}_2$, with the result that a linear supramolecular chain is formed (Figure 13.23c). In the centrosymmetric, tetranuclear cation, $[(dppp)Au_2(^4LH_2)_2Au_2(dppp)]^{4+}$, two $^4LH_2$ bridges are present and these are connected by a 10-membered $\{\ldots HNC_2O\}_2$ synthon within the cavity [40]; dppp is $Ph_2P(CH_2)_3PPh_2$. Further self-association of $^4LH_2$ is precluded by the formation of charge-assisted amide-N–H···O(perchlorate) hydrogen bonds (Figure 13.23d).

The final zero-dimensional structure to be described is that of $[I_2Zn(^4LH_2)ZnI_2]$ [41]. As shown in Figure 13.23e, an oligomeric structure is formed. Owing to severe disorder associated with the co-crystallised methanol molecule, a detailed analysis of

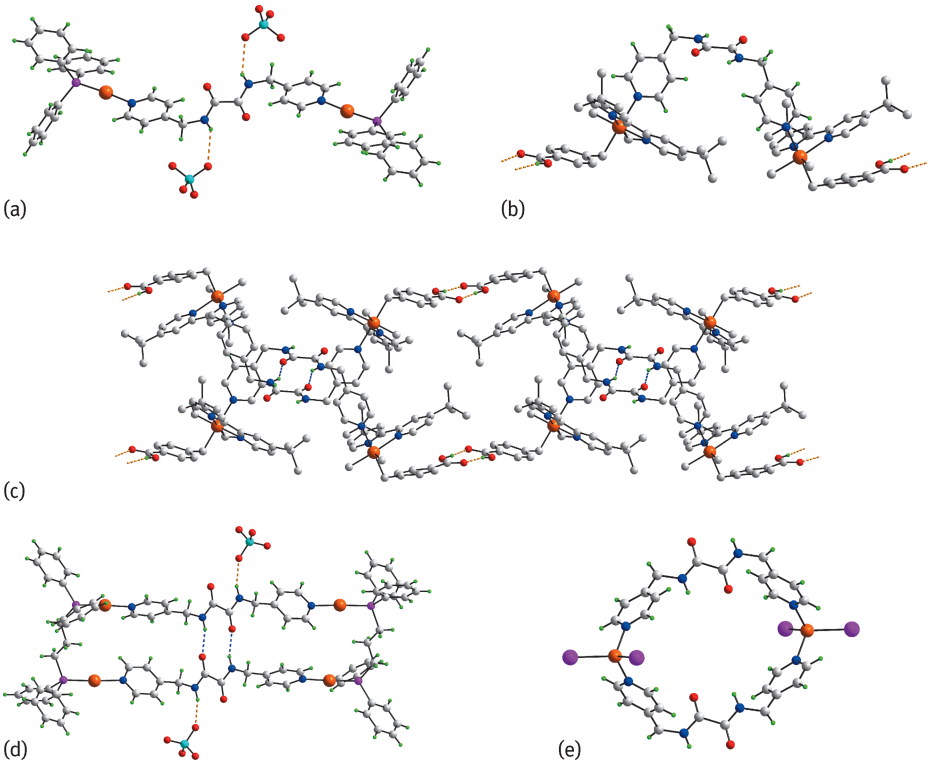

Fig. 13.23: Bidentate bridging modes for [$^4LH_2$] in: (a) {[$Ph_3PAu(^4LH_2)AuPPh_3$][ClO_4]$_2$}, (b) a binuclear platinum(IV) complex (non-$^4LH_2$ hydrogen atoms have been removed), (c) a supramolecular chain whereby the cations in (c) are connected by amide–N···O(amide) and carboxylic acid-O–H···O(carboxylic acid) hydrogen bonds, shown as *blue and orange dashed lines* respectively; non-acidic hydrogen atoms have been removed, (d) {[(dppp)$Au_2(^4LH_2)_2Au_2$(dppp)][ClO_4]$_2$}$^{2+}$ and (e) [$I_2Zn(^4LH_2)ZnI_2$].

the supramolecular association in the crystal is precluded. However, the structure is included here as it varies significantly from the equivalent formulations with either chloride or bromide rather than iodide.

The supramolecular aggregation molecules of the general formula TS.27 [$X_2Zn(^4LH_2)ZnX_2$] is dependent on the nature of X [41]. When X = I, an oligomeric structure is formed (Figure 13.23e). When X = Cl or Br (Figure 13.24a), a zigzag chain is formed with no supramolecular association between chains mediated by $^4LH_2$. A similar zigzag chain is found in [$CoCl_2(^4LH_2)$].½H_2O, where the chain is decorated by the water molecules of crystallisation, which participate in water-O–H···O(amide) hydrogen bonds [9]. In [$Hg_2I_4(^4LH_2)]_n$ (Figure 13.24b), $I_2Hg(^4LH_2)HgI_2$ units are connected into a supramolecular chain via tapes mediated by 10-membered {…HNC_2O}$_2$ synthons [16]. The standout coordination mode for $^4LH_2$ occurs into the

TS.27 Please check: "The supramolecular aggregation molecules … is dependent …"

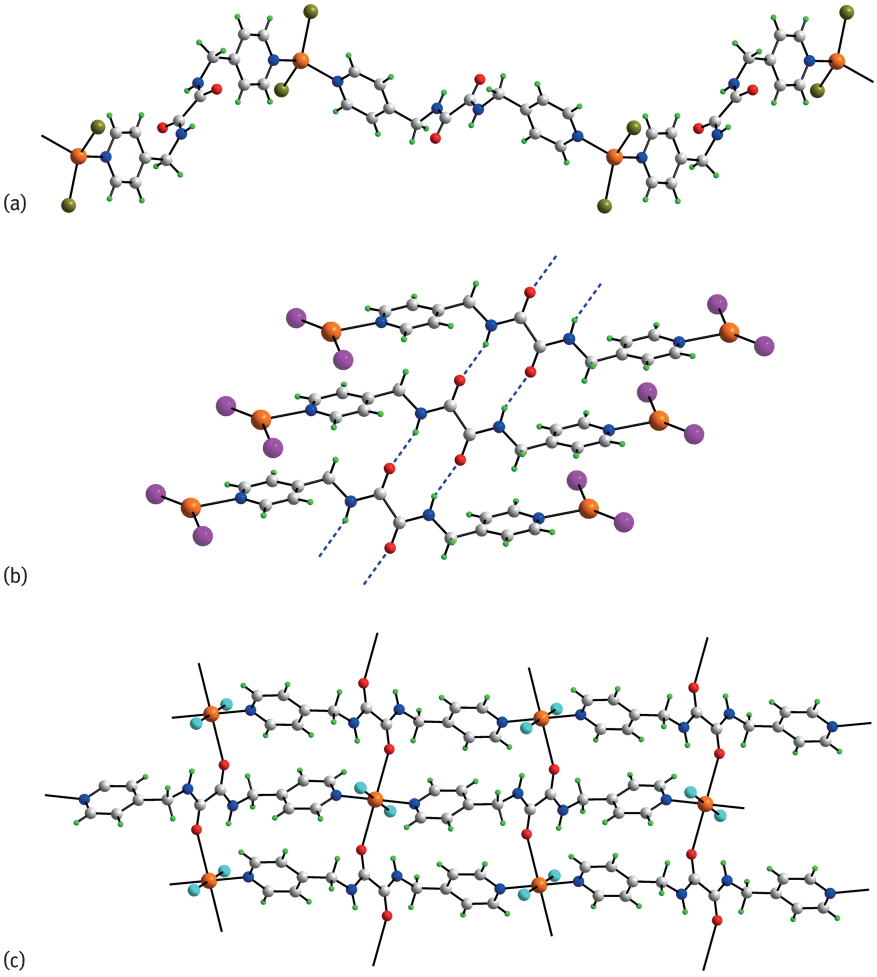

Fig. 13.24: Higher-dimensional aggregation mediated by [$^4LH_2$] in: (a) [$Br_2Zn(^4LH_2)ZnBr_2$], (b) $[Hg_2I_4(^4LH_2)]_n$ in a supramolecular chain connected by amide–N···O(amide) hydrogen bonds shown as *blue dashed lines*, and (c) two-dimensional $[CuCl_2(^4LH_2)]_n$.

two-dimensional structure of $[CuCl_2(^4LH_2)]_n$ [42]. As seen from Figure 13.24c, $^4LH_2$ is bidentate bridging, employing pyridyl-N atoms to generate chains that are linked via Cu–O(amide) bonds indicating a neutral N_2O_2 coordination mode for $^4LH_2$.

The final structure to be described is that of $[Cd_2(NO_3)_4(^4LH_2)_3]_n$ [42]. Each of the three independent and centrosymmetric $^4LH_2$ molecules adopts a bidentate bridging mode of coordination via the pyridyl-N atoms leading to a two-dimensional array shown in Figure 13.25a. The overall architecture is based on mutual orthogonal interpenetration of layers (Figure 13.25b), with the links between the layers being of the type amide-N–H···O(amide) and amide-N–H···O(nitrate) hydrogen bonding.

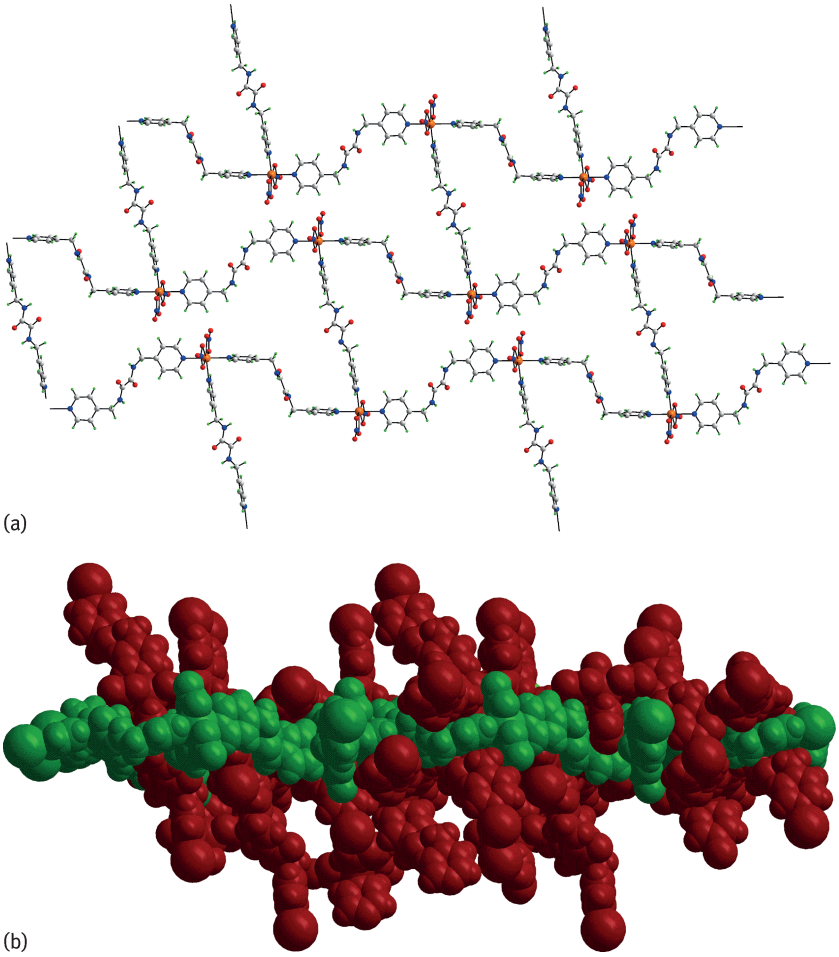

Fig. 13.25: Interpenetration in the structure of $[Cd_2(NO_3)_4(^4LH_2)_3]_n$. (a) View of one two-dimensional array, and (b) orthogonal interpenetration of two arrays, shown in space-filling mode.

13.6 Conclusions and outlook

Herein, it has been demonstrated that $^nLH_2$ and ions derived from these have a high degree of conformational flexibility, engendering these molecules/ions to form disparate supramolecular architectures. In their co-crystals, reliable supramolecular synthons are often formed by $^nLH_2$, e.g. hydroxyl-O–H···N(pyridyl) and amide-N–H···O(amide), with the latter leading to $\{\ldots HNC_2O\}_2$ synthons and often supramolecular tapes. This suggests that targeted co-crystal formation might be feasible for this class of compound. Furthermore, a rich variety of coordination modes are noted for neutral for $^nLH_2$, including monodentate, via pyridyl-N, the common bident-

ate bridging mode, via two pyridyl-N atoms, and even tetradentate modes via two pyridyl-N and two amide-O atoms. For ions derived from these, up to hexadentate coordination modes are possible. This suggests that the relatively unexplored coordination chemistry of $^{n}LH_2$ and their ions are sure to produce exciting discoveries. In summary, this indicates that further investigation of isomeric $^{n}LH_2$ in the context of both multi-component crystals and coordination chemistry is clearly warranted.

Acknowledgement: The support of Sunway University for studies in co-crystals, through Grant No. INT-FST-RCCM-2016-01, is gratefully acknowledged.

Bibliography

[1] Aakeröy C. Is there any point in making co-crystals? Acta Crystallogr B 2015, 71, 387–391.
[2] Duggiral NK, Perry ML, Almarsson Ö, Zaworotko MJ. Pharmaceutical co-crystals: along the path to improved medicines. Chem Commun 2016, 52, 640–655.
[3] Boll G, Nangia A. Pharmaceutical cocrystals: walking the talk. Chem Commun 2016, 52, 8342–8360.
[4] Groom CR, Bruno IJ, Lightfoot MP, Ward SC. The Cambridge Structural Database. Acta Crystallogr B 2016, 72, 171–179.
[5] Spek AL. Single-crystal structure validation with the program PLATON. J Appl Crystallogr 2003, 36, 7–13.
[6] Brandenburg K. DIAMOND. Crystal Impact GbR, Bonn, Germany, 2006.
[7] Jotani MM, Zukerman-Schpector J, Sousa Madureira L, Poplaukhin P, Arman HD, Miller T, Tiekink, ERT. Structural, Hirshfeld surface and theoretical analysis of two conformational polymorphs of N,N′-bis(pyridin-3-ylmethyl)oxalamide. Z Kristallogr 2016, 231, 415–425.
[8] Lee G-H, Wang, HT. Hydrogen-bonded supramolecule of N,N′′-bis(4-pyridylmethyl)oxalamide and a zigzag chain structure of catena-poly[[[dichloridocobalt(II)]-μ-N,N′′-bis(4-pyridylmethyl)oxalamide-κ^2N4:N4′′] hemihydrate]. Acta Crystallogr C 2007, 63, m216–219.
[9] Lee G-H. Hydrogen -bonded supramolecular networks of N,N′′-bis(4-pyridylmethyl)oxalamide and 4,4′′-{[oxalylbis(azanediyl)]dimethylene}dipyridinium dinitrate. Acta Crystallogr C 2010, 66, o241–244.
[10] Zukerman-Schpector J, Sousa Madureira L, Poplaukhin P, Arman HD, Miller T, Tiekink ERT. Conformational preferences for isomeric N,N′′-bis(pyridin-*n*-ylmethyl)ethanedithiodiamides, *n* = 2, 3 and 4: a combined crystallographic and DFT study. Z Kristallogr 2015, 230, 531–541.
[11] Arman HD, Miller T, Tiekink ERT. The robust {C(=O)OH···N(py)} heterosynthon persists in co-crystals formed between anthranilic acid and molecules with amide/pyridyl functionality. Z Kristallogr 2012, 227, 825–830.
[12] Shattock T, Arora KK, Vishweshwar P, Zaworotko, MJ. Hierarchy of supramolecular synthons: persistent carboxylic acid…pyridine hydrogen bonds in co-crystals that also contain a hydroxyl moiety. Cryst Growth Des 2008, 8, 4533–4545.
[13] Jotani M.M, Syed S, Halim SNA, Tiekink ERT. 2-({[(Pyridin-1-ium-2-ylmethyl)carbamoyl]formamido}methyl)pyridin-1-ium bis(3,5-dicarboxybenzoate): crystal structure and Hirshfeld surface analysis. Acta Crystallogr E 2016, 72, 241–248.
[14] Arman HD, Miller T, Poplaukhin P, Tiekink ERT. 2,6-Dinitrobenzoic acid and its 2 : 1 salts formed with isomeric *n*-({[(pyridin-1-ium-*n*-ylmethyl)carbamoyl]formamido}-methyl)pyridin-1-ium, *n* = 2, 3 and 4. Z Kristallogr 2013, 228, 295–303.

[15] Fraser CSA, Eisler DJ, Jennings MC, Puddephatt RJ. Self-assembly of an organometallic side-by-side double helix. Chem Commun 2002, 1224–1225.
[16] Zeng Q, Li M, Wu D, Lei S, Liu C, Piao L, Yang Y, An S, Wang C. Organic-inorganic hybrid aligned by the ligand-ligand hydrogen bonds by using pyridyl-substituted oxalamides as the building blocks. Cryst Growth Des 2008, 8, 869–876.
[17] Arman HD, Miller T, Poplaukhin P, Tiekink ERT. Poly[[bis[μ_2-N,N'-bis(2-pyridylmethyl)oxalamide-$\kappa^4N,O:N',O'$][μ_2-N,N'-bis(2-pyridylmethyl)oxalamide-$\kappa^2N:N'$]disilver(I)] bis(trifluoromethanesulfonate)]. Acta Crystallogr E 2010, 66, m1167–1168.
[18] Reger DL, Smith DMC, Shimizu KD, Smith MD. [N,N′-Bis(2-pyridylmethyl)oxamidato]-palladium(II) monohydrate chloroform hemisolvate. Acta Crystallogr E 2003, 59, m652–654.
[19] Xu L-H, Wang H-X, Zhu, L-N. A new oxamido-bridged dinuclear copper(II) complex with large antiferromagnetic exchange interactions. J Coord Chem 2012, 65, 1051–1061.
[20] Zhang H-X, Kang B-S, Zhou Z-Y, Chan ASC, Chen Zhong-Ning, Ren C. 1-D Structures of assemblies containing oxamidato dicopper building blocks controlled by ditopic N-donor spacers. J Chem Soc Dalton Trans 2001, 1664–1669.
[21] Lloret F, Julve M, Faus J, Journaux Y, Philoche-Levisalles M, Jeannin Y. Oxamidato complexes. 1. A study of the formation of complexes between copper(II) and H_2pmox (H_2pmox = N,N′-bis(2-pyridylmethyl)oxamide). Synthesis, crystal structure, and magnetic properties of the alternating-chain compound $[Cu_2(pmox)(H_2pmox)(H_2O)_2](NO_3)_2.8\,H_2O$. Inorg Chem 1989, 28, 3702–3706.
[22] Syed S, Halim SNA, Jotani MM, Tiekink ERT. A 2 : 1 co-crystal of p-nitrobenzoic acid and N,N′-bis(pyridin-3-ylmethyl)ethanediamide: crystal structure and Hirshfeld surface analysis. Acta Crystallogr E 2016, 72, 76–82.
[23] Arman HD, Miller T, Poplaukhin P, Tiekink ERT. 2,2′-(Disulfanediyl)dibenzoic acid-N,N′-bis(3-pyridylmethyl)ethanediamide (1/1). Acta Crystallogr E 2010, 66, o2590–2591.
[24] Nguyen TL, Fowler FW, Lauher JW. Commensurate and incommensurate hydrogen bonds. An exercise in crystal engineering. J Am Chem Soc 2001, 123, 11057–11064.
[25] Goroff NS, Curtis SM, Webb JA, Fowler FW, Lauher JW. Designed co-crystals based on the pyridine-iodoalkyne halogen bond. Org Lett 2005, 7, 1891–1893.
[26] Jin H, Plonka AM, Parise JB, Goroff NS. Pressure induced topochemical polymerization of diiodobutadiyne: a single-crystal-to-single-crystal transformation. CrystEngComm 2013, 15, 3106–3110.
[27] Jin H, Young CN, Halada GP, Phillips BL, Goroff NS. Synthesis of the stable ordered conjugated polymer poly(dibromodiacetylene) from an explosive monomer. Angew Chem Int Ed 2015, 54, 14690–14695.
[28] Hursthouse MB, Gelbrich T, Plater MJ. Private communication to the CSD, 2003. CSD Refcode: IPOSIP.
[29] Poplaukhin P, Tiekink ERT. Interwoven coordination polymers sustained by tautomeric forms of the bridging ligand. CrystEngComm 2010, 12, 1302–1306.
[30] Li X, He X, Chen Y, Fan X, Zeng, Q. Solid-state supramolecular chemistry of zinc tetraphenylporphyrin and zinc phthalocyanine with bis(pyridyl) ligands. J Mol Struct 2011, 1002, 145–150.
[31] Qin Z, Jennings MC, Puddephatt RJ. Self-assembly in palladium(II) and platinum(II) chemistry: The biomimetic approach. Inorg Chem 2003, 42, 1956–1965.
[32] Zou H, Qi Y. Crystal structure of poly[{μ-N,N′-bis[(pyridin-4-yl)methyl]oxalamide}-μ-oxalato-cobalt(II)]. Acta Crystallogr E 2014, 70, m307–308.
[33] Reger DL, Smith DMC, Shimizu KD, Smith MD. Syntheses and solid state structures of europium and terbium complexes of N,N′-bis(2-pyridylmethyl)urea and N,N′-bis(3-pyridylmethyl)oxalamide. Polyhedron 2004, 23, 711–717.

[34] Arman HD, Kaulgud T, Miller T, Poplaukhin P, Tiekink ERT. Crystal and molecular structures of the 2 : 1 co-crystal of 4-nitrophenylacetic acid and N,N′-bis(pyridin-3-ylmethyl)oxalamide, and with the thioxalamide analogue. J Chem Cryst 2012, 42, 673–679.
[35] Nguyen TL, Scott A, Dinkelmeyer B, Fowler FW, Lauher JW. Design of molecular solids: utility of the hydroxyl functionality as a predictable design element. New J Chem 1998, 22, 129–135.
[36] Curtis SM, Le N, Nguyen T, Xi O, Tran T, Fowler FW, Lauher JW. What have we learned about topochemical diacetylene polymerizations? Supramol Chem 2005, 17, 31–36.
[37] Arman HD, Miller T, Poplaukhin P, Tiekink ERT. 2-[(4-Hydroxyphenyl)diazenyl]benzoic acid–N,N′′-bis(4-pyridylmethyl)oxamide (2/1). Acta Crystallogr E 2009, 65, o3178–3179.
[38] Ouyang X, Fowler FW, Lauher JW. Single-crystal-to-single-crystal topochemical polymerizations of a terminal diacetylene: two remarkable transformations give the same conjugated polymer. J Am Chem Soc 2003, 125, 12400–12401.
[39] Wilhelm C, Boyd SA, Chawda S, Fowler FW, Goroff NS, Halada GP, Grey CP, Lauher JW, Luo L, Martin CD, Parise JB, Tarabrella C, Webb JA. Pressure-induced polymerization of diiodobutadiyne in assembled cocrystals. J Am Chem Soc 2008, 130, 4415–4420.
[40] Tzeng C-C, Yeh H-T, Wu Y-L, Kuo J-H, Lee G-H, Peng S-M. Supramolecular assembly of gold(I) complexes of diphosphines and N,N′-bis-4-methylpyridyl oxalamide, Inorg Chem 2006, 45, 591–598.
[41] Tzeng B-C, Chen B-S, Lee S-Y, Liu W-H, Lee G-H, Peng S-M. Anion-directed assembly of supramolecular zinc(II) halides with N,N′-bis-4-methyl-pyridyl oxalamide. New J Chem 2005, 29, 1254–1257.
[42] Tzeng B-C, Huang Y-C, Chen B-S, Wu W-M, Lee S-Y, Lee G-H, Peng S-M. Crystal-engineering studies of coordination polymers and a molecular-looped complex containing dipyridyl-amide ligands. Inorg Chem 2007, 46, 186–195.